Bioorganic Chemistry 86 (2019) 609–623

Contents lists available at ScienceDirect

Bioorganic Chemistry

journal homepage: www.elsevier.com/locate/bioorg

Design, synthesis, and cytotoxicity screening of 5-aryl-3-(2-(pyrrolyl) thiophenyl)-1, 2, 4-oxadiazoles as potential antitumor molecules on breast cancer MCF-7 cells

Mohammed K. Abd el hameid[a,*], Manal R. Mohammed[b]

[a] Organic Pharmaceutical Chemistry Department, Faculty of Pharmacy, Cairo University, Egypt
[b] Department of Radiation Biology, National Center for Radiation Research and Technology, Cairo, Egypt

ARTICLE INFO

Dedicated to the memory of Dr. Ibrahim Abouleish.

Keywords:
DNA intercalators
Topoisomerase
Thiophene
Oxadiazole
Breast cancer

ABSTRACT

The work representing the design and the cytotoxic screening of synthetic small molecules (SSMs) such as carbonitriles **3a-c**, carboximidamides **4a-c**, and oxadiazoles **5–19** as antitumor molecules. Molecules **4c, 9, 12,** and **14** show promising cytotoxicity profiles against two cell lines higher than prodigiosin (PG). The results of topoisomerase enzyme inhibition assay show that compounds **4c** and **14** display potent inhibitory activity in nano-molar concentration. In addition, DNA-flow cytometry and annexin V analysis also display that compounds **4c**, **9**, **12**, and **14** exhibit antiproliferative activities over MCF-7 cells by cell cycle arrest at G_1 phase and apoptosis-inducing activity by increasing cell percentages at pre G_1 phase. Moreover, Elisa measurement of p53 and apoptosis mediators, show that carboximidamide **4c** and oxadiazoles **9**, **12**, and **14** significantly up-regulate p53 and cell death mediators as puma and Bax/Bcl-2 ratio levels. Subsequently, pro-apoptotic activities are confirmed by active caspase 3/7 percentages green fluorescence assay.

1. Introduction

DNA synthesis has been regarded as one of the most effective targets in cancer cell growth inhibition and apoptosis induction [1]. Generally, all cancer cells are characterized by increasing DNA synthesis that has been mainly referred to up-regulation of DNA topoisomerase (topo) enzymes. Mechanistically, DNA interactive molecules exert their mode of action as DNA intercalators and topo inhibitors or by dual mode of action actions. Structurally, the common structural basis for DNA synthesis inhibitors is the polycyclic molecular skeleton either orthogonal or planar that required for DNA base pair interaction. Besides that, the molecular skeletons also have to carry side chains that anchor DNA base pairs or enzyme binding sites by non-covalent interaction [2]. Natural products are important utility in drug discovery as the diversity of their structures inspires the discovery of many drugs [3]. Terthiophene (TER), terpyridine and prodigiosin (PG) (Fig. 1) are natural compounds with an orthogonal tri-arylated molecular skeleton and exhibit potent cytotoxic and pro-apoptotic properties toward a variety of cancer cell lines. The mode of action of these compounds is mainly DNA synthesis inhibition [4–8]. Obatoclax (*Teva Pharmaceuticals*) (Fig. 1) is an apoptotic inducer agent in clinical trials over different cancer cell lines and is synthetically derived from prodigiosin [8].

The oxazole, isoxazole and oxadiazole rings are a privileged core in numerous antitumor molecules like MX 74420(*Maxim Pharmaceuticals*), SEW 2871(*EPI Corporation*), VA-62784 and molecule I (Fig. 1) [9–13]. Interestingly, oxadiazole derivatives exhibited promising antitumor activities with different modes of actions [14–18]. The mentioned heterocyclic rings represent promising scaffolds in the design of DNA interacting agents due to the following reasons. They have a similar configurational ability to act as a rigid spacer between two pharmacophoric arms. In addition, these rings are hydrogen bond (H-bond) acceptor (A) forming moieties that facilitate binding with DNA and enzyme binding sites [19]. The mentioned cytotoxic molecules show a common configurational resemblance in their molecular structures as curved or orthogonal poly-aryl ring system composed of a core part equipped with two symmetrical or unsymmetrical aryl groups as side chains. The resistance of cancer cells to apoptosis induction by antitumor drugs is appeared mainly due to dysfunction in tumor suppressor gene (p53) and up-regulated expression of cell death modulators as the Bcl-2 protein family [20]. P53 upregulated modulator of apoptosis (puma) is a downstream protein of p53 and is expressed as a secondary effect of DNA damage to induce apoptosis in cancer cells. Puma plays a crucial role in the determination of the Bax/Bcl-2 ratio level in the cancer cells [21]. The resistance of cancer cells to apoptosis induction

* Corresponding author.
E-mail address: mohamed.sayed@pharma.cu.edu.eg (M.K. Abd el hameid).

https://doi.org/10.1016/j.bioorg.2019.01.067
Received 18 August 2018; Received in revised form 9 January 2019; Accepted 30 January 2019
Available online 31 January 2019
0045-2068/ © 2019 Elsevier Inc. All rights reserved.

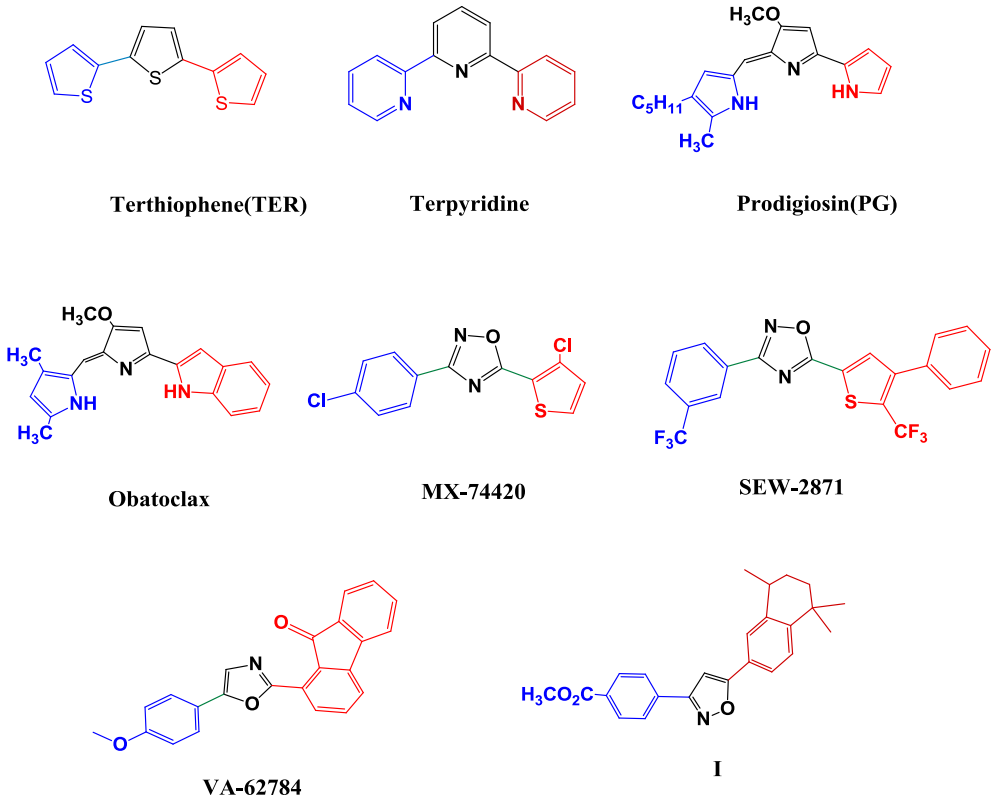

Fig. 1. Chemical structure of antitumor agents as orthogonal tricyclic molecules. Core rings is are shown in black color, bulky aryl groups are in red color and other small aryl groups are in blue color.

for the chemotherapy is appeared mainly to be due to dysfunction in tumor suppressor gene (p53) and up-regulated expression of cell death modulators such as the Bcl-2 protein family. Therefore, the discovery of novel antitumor molecules enhancing apoptosis-inducing activities represents a significant challenge in the oncology research.

Based on these aforementioned structural similarities and a bioisosteric relation between benzene, thiophene and azole rings, synthetic small molecules (SSMs) are designed as antitumor agents using the utility of fragment-based drug design strategy (Fig. 2). The basic structural skeleton of the lead template is formed from orthogonal 2-(pyrrol-1-yl) thiophene-3-carbonitrile **3a-c**. In addition, thiophene fragments are decorated at C-4 and C-5 positions with three different lipophilic and conformational moieties as dimethyl and tetra-methylene and 4-methoxyphenyl groups to give variable skeletal extensions. Furthermore, the thiophene-3-carbonitriles **3a-c** are grafted with a carboximidamide group as (H-bond) acceptor-donner (A-D) pair forming group via chemical modification of carbonitrile group to reinforce the interaction with the DNA and/or the enzyme. Besides that, a carboximidamide group also is capable of forming a pseudo intramolecular H-bond ring that extended the structural skeleton (model A, the carboximidamides **4a-c**). Finally, the amidoxime group in the conformers **4a-c** is rigidified into oxadiazole with the addition of aryl side chain at the C-5 of the core (model B, oxadiazoles **5–19**). The final molecules **5–19** are formed from 3, 5-diaryl oxadiazole skeleton with oxadiazole as core ring and unsymmetrical C-3 and C-5 diaryl groups, C-3 moieties are equipped with 2-(pyrrol-1-yl) thiophen-3yl fragments as bulky side chains and C-5 moieties are substituted phenyl groups) (Fig. 2).

2. Discussion

2.1. Chemistry

The steps for the synthesis of starting materials, intermediates and the target compounds **3a-c, 4a-c** and **5–19** are illustrated in Schemes 1–3. The rationale of using microwave-assisted organic synthesis (MAOS) in the synthesis of organic molecules is to create a green road towards sustainable development in the chemical industry [22]. Open vessel microwave-assisted synthesis (OVMAS) could be used in the large-scale synthesis and, therefore is suitable for industry [22]. Since Gewald reported his synthetic protocol for the preparation of 2-aminothiophenes from ketones, active methylene derivatives and sulfur, several reports were published to improve the reaction conditions [23–26]. In the current work, 2-aminothiophenes **2a-c** were prepared in three component reaction via reacting ketones **1a-c** with propane dinitrile and sulfur with using morpholine as a catalyst in *n*-butanol, (high boiling solvent), instead of ethanol under OVMAS conditions (Scheme 1). The structure of thiophene derivatives **2a-c** was confirmed by their reported physical and spectral data [23–25]. Synthesis of pyrrole ring from primary amines using dimethoxytetrahydrofuran (DMTHF) under acid catalyst was known as Clauson-Kaas reaction [27]. In the current work, 2-(pyrrol-1-yl) thiophenes **3a-c** were prepared by reacting 2-aminothiophenes **2a-c** with DMTHF in acetic acid as a dual solvent and catalyst under OVMAS conditions (Scheme 1). Thiophene **3a** was reported as a patent molecule [28], while 2-(pyrrolyl) thiophene **3b** is known in the literature by synthesis under conventional heating with incomplete structural characterization [29]. The synthesis of 1, 2, 4-oxadiazole ring was reported from the reaction of carbonitrile, hydroxylamine and acylating agents as carboxylic acids and acid derivatives. The reaction sequence involves the following mechanistic steps, the hydroxylamine was added to aryl nitriles to form amidoximes under base catalyzed conditions. After that, the amidoximes were coupled with the acylating agents to form oxadiazole ring [30–32]. In this work, oxadiazoles **5–19** (Fig. 3) were prepared by reacting thiophene-3-carbonitriles **3a-c** with hydroxylamine hydrochloride using cesium carbonate as a catalyst instead of potassium carbonate, (unstable in M.W irradiation), in *n*-butanol under OVMAS conditions to produce thiophene-3-carboximidamides **4a-c** (Scheme 2).

The structure of novel amidoximes **4a-c** was established using IR,

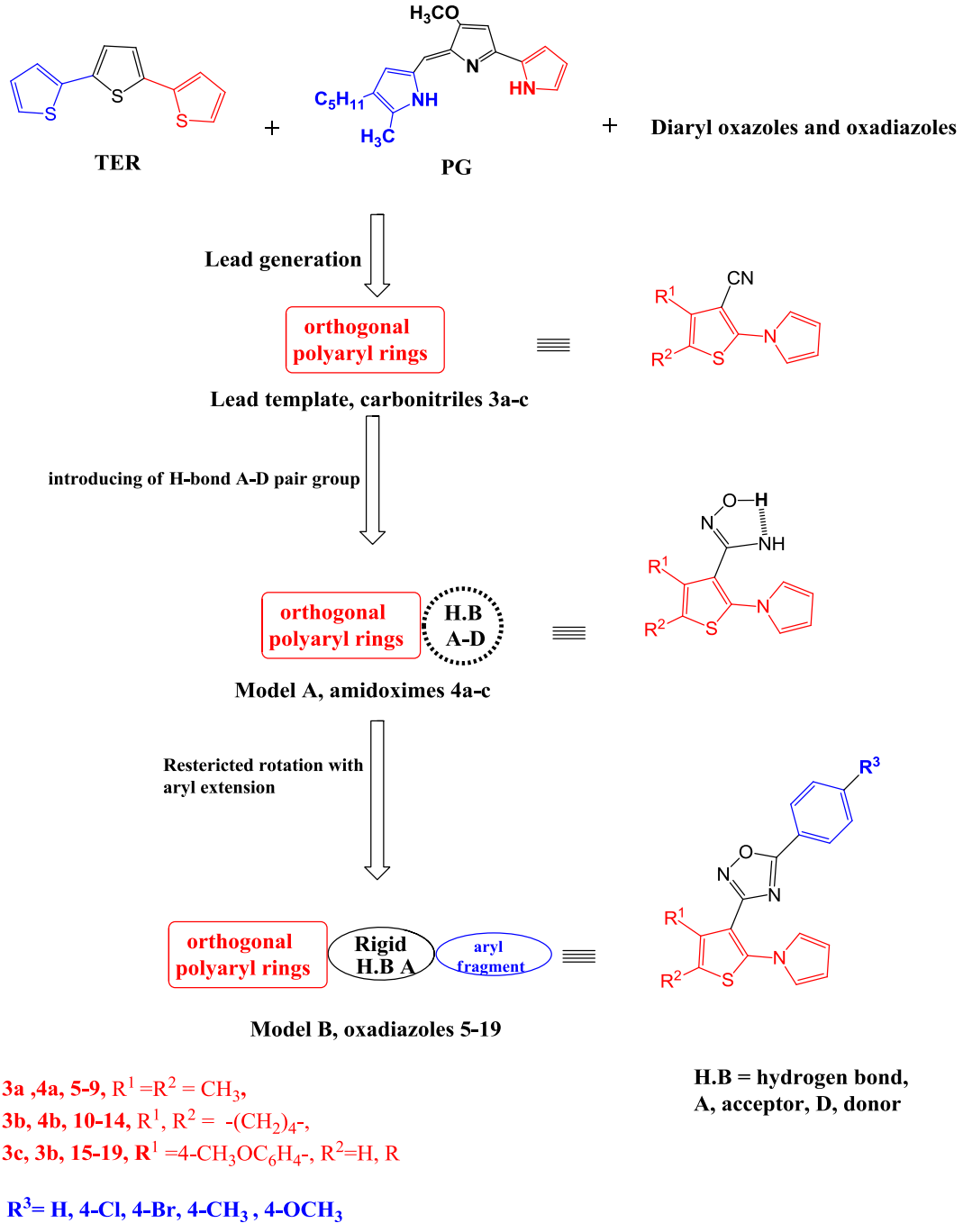

Fig. 2. Diagrammatic sketch illustrate the design strategy. Orthogonal substituted polyaryl lead moieties are shown in red color, H-bond forming group and rigid oxadiazole core ring are in black color and small aryl fragments at C-5 of the core are in blue color.

NMR spectroscopy, in IR spectra of carboximidamides **4a-c**, they show absence of absorption band at 2218 cm^{-1} characteristic to nitrile group cm^{-1} and appearance of absorption bands at the range 3413–3041 cm^{-1} corresponding to NH_2 and OH groups, while ^1H NMR confirm the presence of signals of NH_2 and OH at 4.90–4.95 and 10–63-10.77 ppm. In the second step, amidoximes **4a-c** were acylated with appropriate acid chlorides in ethylene glycol (high boiling solvent) under OVMAS conditions to give 3,5-diaryl 1, 2, 4-oxadiazoles **5–19** (Scheme 3). Several synthetic trails were performed to prepare oxadiazoles **10–14** from the nitrile **3b**, hydroxylamine, cesium carbonate and acid chlorides in three-component reaction conditions but the results of all synthetic trails produced the amide of corresponding nitrile **3b**.

2.2. *In vitro anti-proliferative studies*

2.2.1. *In vitro cell growth inhibition*

The molecules **3a-c**, **4a-c,** and **5–19** are evaluated for anti-proliferative activity against breast cancer MCF-7 cell line using MTT assay [33] and prodigiosin (PG) is used as positive control [7,8]. The obtained results are shown in (Table 1 and Fig. 4).

Carboximidamides **4b**, **4c** and oxadiazoles **9**, **11**, **12**, and **14** with IC_{50} less than (5 μM) against MCF-7 cells were selected for further cytotoxic evaluation on human colon cancer HCT-116 cell lines. The results over MCF-7 cells show that SSMs **4c, 9, 12,** and **14** exhibited cytotoxic activity in sub-micromolar concentration (IC_{50}: 0.19–0.83 μM). Inspection of the results according to structural

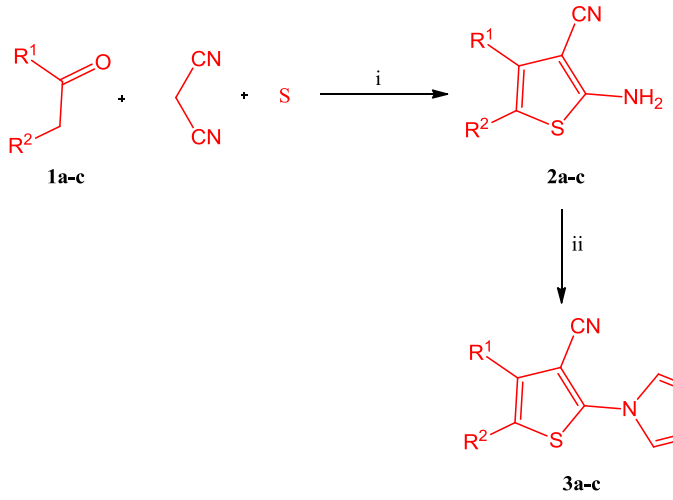

2a) R^1, R^2= CH_3 2b) R^1, R^2=-$(CH_2)_4$- 2c) R^1= 4-$CH_3OC_6H_4$, R^2= H

3a) R^1, R^2= CH_3, yield=74 % 3b) R^1, R^2=-$(CH_2)_4$-, yield=81 % 3c) R^1= 4-$CH_3OC_6H_4$, R^2= H, yield=76 %

Reagents & conditions: i) *n*-butanol, morpholine, 150^0 C , M.W, 10 min.
ii) DMTHF, acetic acid, 100^0 C , M.W, 15 min.

Scheme 1. Synthesis of 2-aminothiophenes **2a-c** and 2-(pyrrol-1-yl) thiophene-3-carbonitriles **3a-c**.

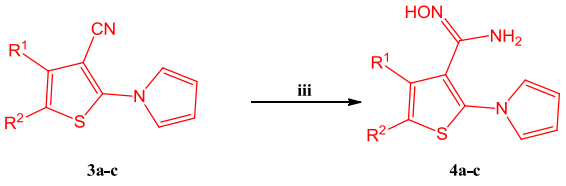

4a) R^1, R^2= CH_3, yield = 59%
4b) R^1, R^2=-$(CH_2)_4$-, yield = 67%
4c) R^1=4-$CH_3OC_6H_4$, R^2= H, yield = 58%

Reagents & conditions: iii) $NH_2OH.HCl$, K_2CO_3, *n*-butanol, 140 ^{0}C , M.W, 20 min.

Scheme 2. Synthesis of 2-(pyrrol-1-yl) thiophene-3-carboximidamides **4a-c**.

variations between the molecules showed the following remarks. Structural modification of thiophene −3-carbo nitrile **3a-c** into thiophene-3-carboximidamides **4a-c** led to improvement in cytotoxicity results, that may be explained by increasing hydrogen bond formation. Regarding groups present at C-4 and C-5 of thiophene ring, carbonitrile **3c** and carboximidamide **4c** exhibited higher activity within SSMs **3a-c** and SSMs **4a-c,** indicating that common C-4 (4-methoxyphenyl) has more contribution in the cytotoxicity than the other two groups. Meanwhile, in model B, 3-(tetrahydrobenzothiophenyl) oxadiazoles **11, 12,** and **14** displayed higher cytotoxicity among oxadiazoles **5–19**, suggesting that tetra-methylene group at thiophene ring has higher cytotoxicity compared with other C-4 and C-5 substituents at thiophene ring. Also, restriction of rotation in amidoxime moiety in thiophene-3-carboximidamides **4a-c** with the addition of different aryl extension may lead to an increase in cytotoxicity as oxadiazoles **10–14** or decrease in cytotoxic activity as in SSMs 1**5–19**. In respect to the C-5 aryl groups of oxadiazoles **5–19**, SSMs **9, 11, 12** and **14** are the most cytotoxic compounds, indicating that 4-methoxyphenyl, 4-chlorophenyl, and 4-bromophenyl have a positive effect on cytotoxicity. Interestingly, the molecular skeleton of 3,5-diaryl oxadiazoles **5–19** tolerates only one 4-methoxyphenyl group for good cytotoxic activity. This observation was confirmed by the low cytotoxicity results exhibited by SSMs **15–19**, where their precursor **4c** is a potent cytotoxic agent. In respect to sensitivity of MCF-7 and HCT-116 cells toward the tested molecules, MCF-7 cells were more sensitive than HCT-116 cells to the tested compounds, except 4**c** (as indicated by the IC_{50} values). Moreover, thiophene-3-carboximidamide **4c** is more potent than oxadiazole **14** and PG by 2.1- and 4.96- fold over HCT-116 cells. Besides that, oxadiazoles **12** and **14** with C-5 4-bromophenyl and 4-methoxyphenyl groups exhibited good cytotoxic effect over HCT-116 cells. According to these observations, it is concluded that an orthogonal tri- and tetra-orthogonal aryl molecules **4c** and **14** have antitumor activity over both cell lines.

2.2.2. In vitro topoisomerase inhibition assay

Further topo 2β enzymatic inhibition at 5 different doses was performed for the selected molecules carboximidamide **4b**, **4c** and oxadiazoles **9, 11, 12,** and **14** to evaluate their topo 2β IC_{50} values using PG as a reference. The results are presented in (Table 1 and Fig. 5). The results show that SSMs **4c**, **9**, **12**, and **14** were more potent topo inhibitors than control that correlate the cytotoxic activity of the compounds to topo enzyme inhibition. In respect to structural activity correlation, 4-(4-methoxyphenyl) thiophene **4c** displayed higher topo inhibition than tetrahydrobenzothiophene **4b** indicating that, 4-methoxyphenyl is more active than tetramethylene group at thiophene ring in enzyme inhibition in respect to model A. In addition, oxadiazole **14** is more enzyme inhibitor than carboximidamide **4b** by 4.6- fold, suggesting that, the rigid model B displayed higher activity than rotatable model A. Furthermore, 3-(tetrahydrobenzothiophenyl) oxadiazole **14** showed higher topo enzyme inhibition than 3-(4,5-dimethylthiophenyl) oxadiazole **9**, indicating that tetra-methylene group shows higher activity than dimethyl moieties at thiophene ring in model B. Although 4-(4-methoxphenyl) thiophene −3-carboximidamide **4c** and 5-(4-methoxyphenyl) oxadiazole **9** are from different models they were nearly equipotent in topo inhibition, that confirm the role of the 4-methoxyphenyl group in the enzyme inhibition activity. Oxadiazole **14** with C-5(4-methoxyphenyl) group was more potent than other oxadiazoles **11** and **12** with C-5 (chlorophenyl and bromophenyl), confirming the previous finding. Finally, 5-(4-bromophenyl) oxadiazole **12** exhibited higher enzyme inhibition than 5-(4-chlorophenyl) oxadiazole **11,** indicating that the halide nature contributes to enzyme inhibition activity.

2.2.3. In vitro DNA immunofluorescence assay

On structural basis for SAR studies, carboximidamide **4b**, **4**c and oxadiazoles **9**, and **14** were selected for DNA binding affinity compared

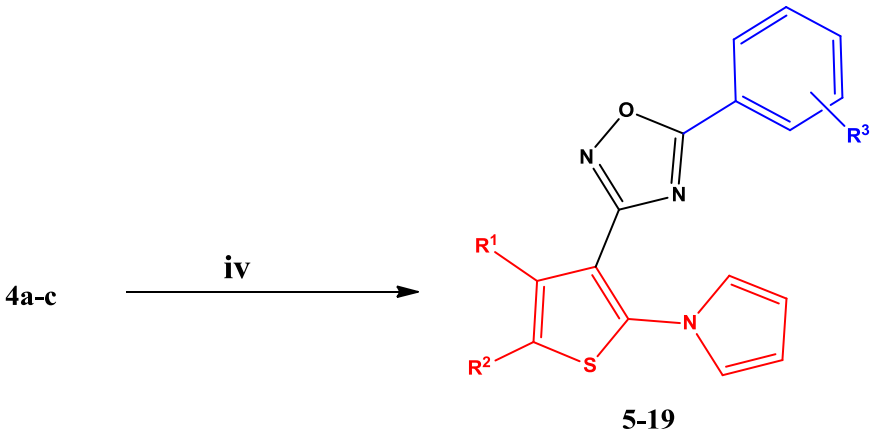

5) R^1=R^2= CH_3, R^3=H, yield=75 %

6) R^1=R^2= CH_3, R^3=4-Cl, yield=55 %

7) R^1=R^2= CH_3, R^3=4-Br, yield=59 %

8) R^1=R^2= CH_3, R^3=*4*-CH_3, yield=49 %

9) R^1=R^2= CH_3, R^3=4-OCH_3, yield=56 %

10) R^1&R^2=-$(CH_2)_4$-, R^3=H, yield=79 %

11) R^1&R^2=-$(CH_2)_4$-, R^3=*4*-Cl, yield=63 %

12) R^1&R^2=-$(CH_2)_4$-, R^3=4-Br, yield=66 %

13) R^1&R^2=-$(CH_2)_4$-, R^3=4-CH_3, yield=60 %

14) R^1&R^2=-$(CH_2)_4$-, R^3=4-OCH_3, yield=58 %

15) R^1= 4-$CH_3OC_6H_4$, R^2= H, R^3=H, yield=71 %

16) R^1= 4-$CH_3OC_6H_4$, R^2= H, R^3=4-Cl, yield=59 %

17) R^1= 4-$CH_3OC_6H_4$, R^2= H, R^3=*4*-Br, yield=65 %

18) R^1= 4-$CH_3OC_6H_4$, R^2= H, R^3=4-CH_3, yield=58 %

19) R^1= 4-$CH_3OC_6H_4$, R^2= H, R^3= 4-OCH_3, yield=46 %

Reagents & conditions :iv , acid chloride, ethylene glycol, 200 C^0 , M.W, 5 min.

Scheme 3. Synthesis of 5-aryl-3-(2-(1H-pyrrol-1-yl)-thiophen-3-yl) 1, 2, 4-oxadiazoles **5–19**.

with PG, indirect binding pico -green immunofluorescence assay was performed (Fig. 6). In this assay, the fluorescent pico-green dye reversibly binds DNA to form a persistent fluorescent colored complex. When the DNA intercalators are added, the dye is displaced from DNA leading to a decrease in fluorescence [34]. The results showed that model A (SSMs **4b** and **4c**) had good binding affinity than model B (**9** and **14**). The obtained results exhibited a difference from the results of structural correlation between cytotoxicity, topo enzyme inhibition assay that may be referred to good abilities of **4b** and **4c** to form a higher hydrogen bond with DNA base pair and hence have bitter DNA binding activity than **9** and **14**.

2.2.4. In vitro DNA- flow cytometry and Annexin V/PI staining analysis

To explore the effect of molecules **4b**, **4c**, **9,** and **14** on cell growth inhibition and pro-apoptotic characters, the molecules were subjected to DNA flow cytometry cell cycle analysis. The results are shown and summarized in (Fig. 7). The distribution pattern of cell cycle phases for MCF-7 cells is a significantly changed after incubation with tested molecules at their IC_{50} compared with PG and untreated cells [35]. The molecules induced a significant accumulation percentage of the cells in G_0 phase by 8-, 13-, 9.5- and 15 - fold and G_2/M phases by 1.4-, 1.8-, 1.5- and 1.8- fold respectively, compared with untreated cells, indicating that the tested molecules have cell cycle arrest at G_1 phase and pro-apoptotic activities. In addition, only, SSMs **4c**, **14** and PG induced

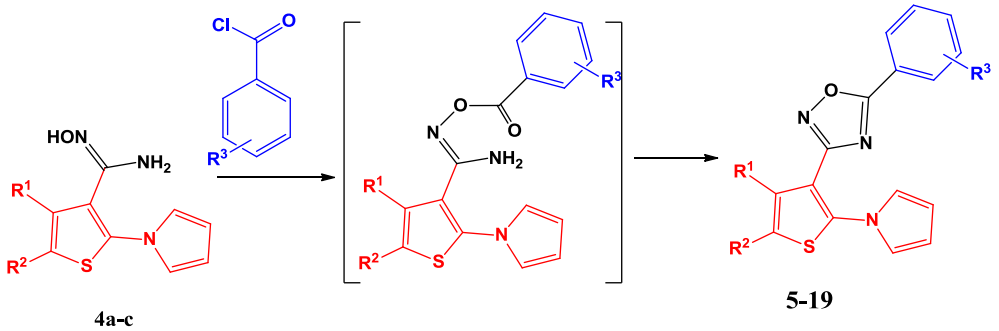

R^1, R^2 = 2 CH_3,- $(CH_2)_4$-, H, 4-CH_3O-C_6H_4

R^3 = H, Cl, Br, CH_3, OCH_3

Fig. 3. Sketch diagram represent the mechanism of formation of 3,5-diaryl oxadiazoles **5–19** from amidoximes **4a-c**.

Table 1
IC_{50} of carbonitriles **3a-c**, carboximidamide **4a-c** and oxadiazoles **5–19** on MCF-7 cells (μM) and topo enzyme (nM).

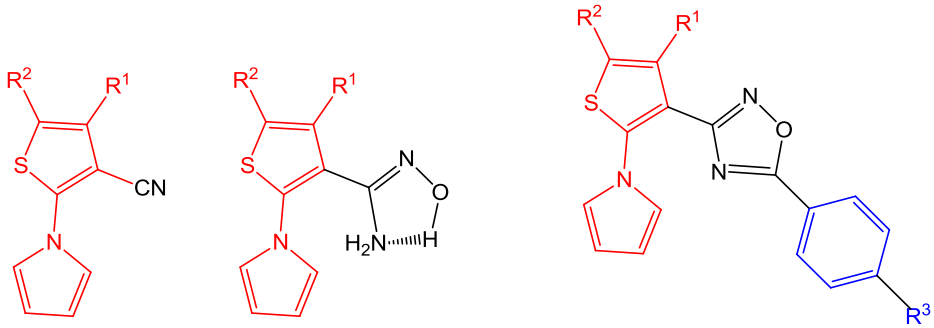

Code	R^1	R^2	R^3	MCF-7[a]	HCT-116[b]	Topo[c]
				IC_{50} (μM)[d]		IC_{50} (nM)[e]
3a	$-CH_3$	$-CH_3$	-	19.45 ± 1.61	NT	NT
3b	$-(CH_2)_4-$		–	16.10 ± 1.10	NT	NT
3c	4-$CH_3OC_6H_4$	H	–	13.40 ± 1.18	NT	NT
4a	$-CH_3$	$-CH_3$	–	5.98 ± 0.41	NT	NT
4b	$-(CH_2)_4-$		–	4.52 ± 0.43	10.52 ± 1.03	123.49 ± 9.41
4c	4-$CH_3OC_6H_4$	H	–	0.83 ± 0.06	0.57 ± 0.06	35.32 ± 4.08
5	$-CH_3$	$-CH_3$	H	13.43 ± 0.91	NT	NT
6	$-CH_3$	$-CH_3$	4-Cl	9.82 ± 0.47	NT	NT
7	$-CH_3$	$-CH_3$	4-Br	8.64 ± 0.81	NT	NT
8	$-CH_3$	$-CH_3$	4-CH_3	12.43 ± 1.46	NT	NT
9	$-CH_3$	$-CH_3$	4-OCH_3	0.48 ± 0.07	5.13 ± 0.26	36.31 ± 1.16
10	$-(CH_2)_4-$		H	12.94 ± 0.92	NT	NT
11	$-(CH_2)_4-$		4-Cl	1.98 ± 0.09	2.51 ± 0.53	87.46 ± 9.21
12	$-(CH_2)_4-$		4-Br	0.78 ± 0.06	1.54 ± 0.08	69.56 ± 1.14
13	$CH_2)_4-$		4-CH_3	10.51 ± 0.82	NT	NT
14	$-(CH_2)_4-$		4-OCH_3	0.19 ± 0.05	1.17 ± 0.09	27.28 ± 1.11
15	4-$CH_3OC_6H_4$	H	H	13.76 ± 1.10	NT	NT
16	4-$CH_3OC_6H_4$	H	4-Cl	12.11 ± 1.11	NT	NT
17	4-$CH_3OC_6H_4$	H	4-CH_3	15.22 ± 1.32	NT	NT
18	4-$CH_3OC_6H_4$	H	4-Br	15.62 ± 1.31	NT	NT
19	4-$CH_3OC_6H_4$	H	4-OCH_3	21.80 ± 1.71	NT	NT
PG	–	–	–	1.93 ± 0.18	2.84 ± 0.26	73.14 ± 6.23

MCF7, [a] Human breast, HCT116, [b] Human colon cancer cell lines, Topo[c], topoisomerase 2β enzyme, d, values are expressed as + SEM (n: 3) in micromolar concentration and e, values mean + SEM (n = 3) in nanomolar concentration, NT - Not tested.

a significant decrease in the cell population at S phase by 2 -, 1.6- and 1.3- fold respectively, compared with untreated cells. It could be concluding that, tested molecules **4c** and **14** exhibited potent anti-proliferative activity than compounds **4b** and **9**.

The annexin-V/PI double staining assay further confirm that apoptosis events occurred in MCF-7 cells. The results were shown and summarized in (Fig. 8). Results of the assay showed both stages of apoptotic MCF-7 cells increase by **4b**, **4c**, **9,** and **14** by 8 -, 11-, 9 -, and 15 - fold compared with untreated cells. Moreover, SSM **14** exhibited a profile of strong apoptotic inducer over MCF-7 cells by 1.2- fold than PG. In conclusion, data indicate that SSM **4b**, **4c**, **9,** and **14** were a potent inducer of apoptosis over MCF-7 cells and compound **14 could** induce apoptosis percentage higher than PG, SSM **4c** was slightly less potent than PG, meanwhile SSMs **4b** and **9** showed equal apoptotic inducing activity to each other and lower than PG.

2.2.5. In vitro ElISA immunoassay for p53 and cell death modulators

P53 is the main regulator of the intrinsic apoptotic pathway induced by different stimulations via expression of Puma. Therefore, ELISA-immunoassay for p53, puma, Bax and Bcl-2 measurement in MCF-7 cells for the effect of molecules **4b**, **4c**, **9,** and **14** at their IC_{50} compared with untreated cells and PG is performed. The results were presented in (Fig. 9A–E). The data indicated that SSMs **4b**, **4c**, **9,** and **14** up-regulated p53 levels by 12-, 17-, 19.5-, and 25.7- fold, respectively, higher than untreated cells (Fig. 9A). Molecules **4c** and **9** were nearly equivalent in their up-regulation and both are less than **14** and PG. Molecule **14** increased p53 level by 1.1- fold higher than PG. Similarly, SSMs **4b**, **4c**, **9,** and **14** increased puma level by 4.5-, 6.5-, 5-, and 7.0-, fold, respectively more than untreated cells (Fig. 9B). Meanwhile, SSM **14** increased level of puma higher than PG by 1.2-fold and **4c** is equipotent compound to PG. This increasing in p53 and puma levels most probably caused by DNA damage effect of the tested compounds.

Subsequently, to increase in p53 and puma levels, the data showed that, an increase in Bax and a decrease in Bcl-2 levels (Fig. 9C, D and E). Compounds **4b, 4c**, **9,** and **14** increase Bax/Bcl-2 ratio by 4.3-, 8.5-, 3.5, and 9.5- fold to untreated cells. SSM **14** has higher Bax/Bcl-2 ratio by 1.3-fold than PG (Fig. 9E). The data obtained from p53, puma and Bax/Bcl-2 ratio support the previous elucidated structure activity correlation between the tested compounds.

2.2.6. In vitro green flow cytometry assay for active caspase 3/7

Caspase-3/7 enzymes are the terminal downstream of caspases activation that catalyzed the apoptosis process either intrinsic or extrinsic pathways. Treated MCF-7 cells with compounds **4b, 4c, 9, 14,** and PG at their IC_{50} are subjected to green immunofluorescence to measure active caspase-3/7 percentages. The data show that carboximidamides

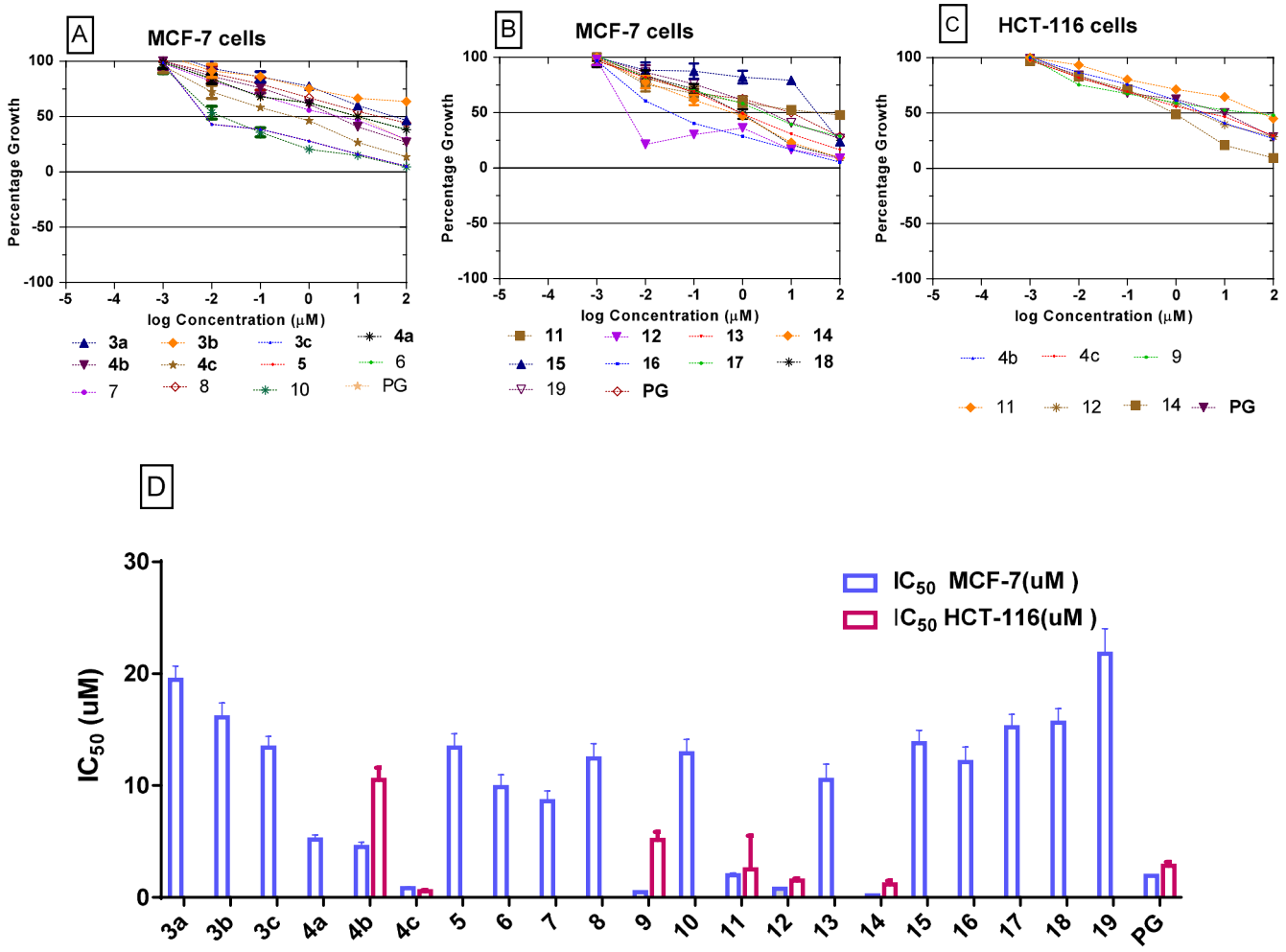

Fig. 4. Dose response curves for cell percentage viability of MCF-7cells, HCT-116 cells after treatment with tested molecules determined by MTT assay. (A & B) Growth Inhibition effect of molecules on MCF-7 cells, (C) Growth Inhibition effect of tested molecules on HCT-116 cells, (D) Graphical presentation of the IC_{50} of tested molecules. Data is shown as mean SEM (n: 3).

4b,**4c** and oxadiazoles **9, 14** increased active caspase-3/7 percentages by 3-, 8.6-, 6.4-, 10-fold, respectively, more than untreated MCF-7 cells as seen in (Fig. 10). Additionally, carboximidamide **4c** increased caspase 3/7 higher than oxadiazole **9**. Moreover, carboximidamide **4c** and oxadiazole **14** increased caspase-3/7 percentages by 1.1- and 1.3- fold than PG. As a final conclusion from biological screening results, molecules **4b**, **4c**, **9,** and **14** are cytotoxic agents and trigger apoptosis induction in MCF-7 cells as a secondary effect to DNA damage with subsequent secondary increasing in p53 and Puma levels that overcome the resistance conferred by Bcl-2 proteins via an increase in Bax/Bcl-2 ratio and activation of terminal caspase 3/7 proteins.

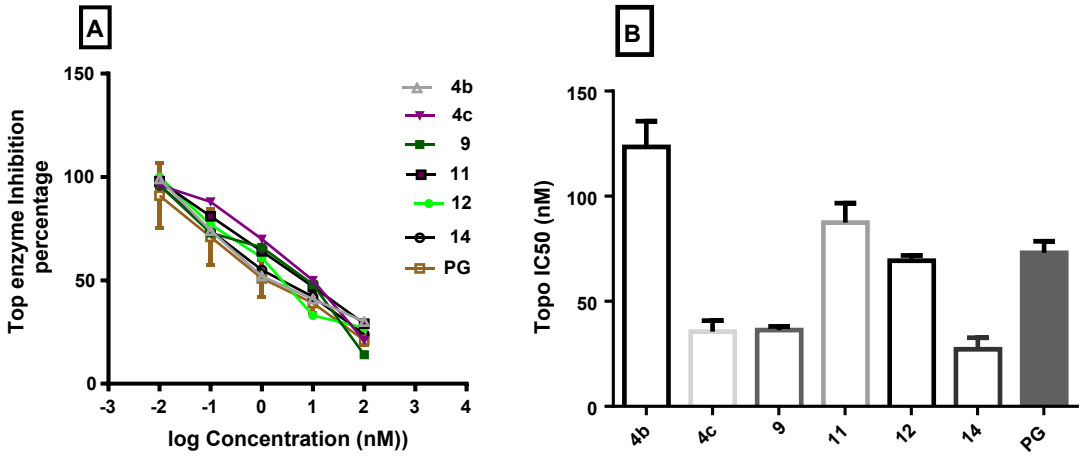

Fig. 5. (A) In vitro 5 dose response curve for the determination of topo 2- β enzyme IC_{50} (nM) for SSMs **4b**, **4c**, **9**, **11**, **12**, **14** compared with PG, (B) Graphical presentation for comparison of IC_{50} for topo 2- β enzyme (nM) of the tested molecules and PG. the obtained data and are expressed as mean (n: 3) ± SEM.

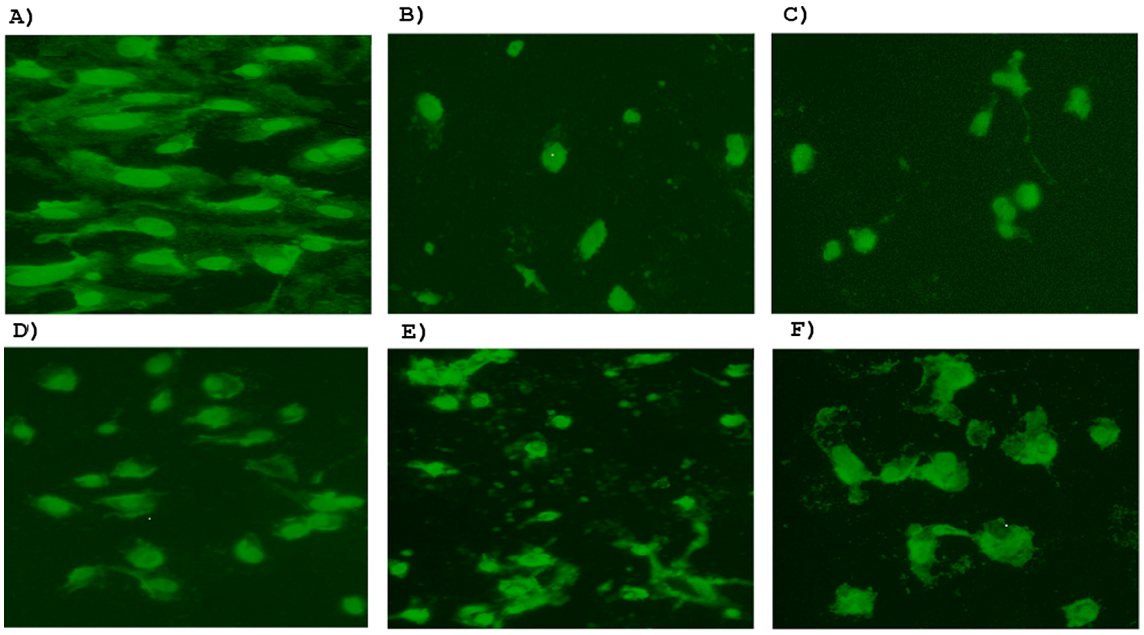

Fig. 6. Fluorescence intensity (IFU) of DNA indirect binding assay in MCF-7 cells for the effect of compounds **4b**, **4c**, **9** and **14** at their IC_{50} compared with PG as control for 24 h. (A) Untreated cells, (B) Cells treated with of **4b** (4.52 μM), (C) Cells treated with SSM **4c** (0.83 μM), (D) Cells treated with SSM **9** (0.48 μM), (E) Cells treated with SSM **14** (0.19 μM), (F) Cells treated with PG (1.93 μM).

3. Conclusion

Briefly, a small library of carbonitriles **3a-c**, carboximidamides **4a-c** and oxadiazoles **5–19** is designed as potential anticancer molecules. The following steps demonstrate the synthetic protocol, where thiophene derivatives **2a-c** are synthesized in three component Gewald reaction. In addition, the amino group of thiophene-3-carbonitrile **2a-c** is cyclized into pyrrole ring (thiophenes **3a-c)** using DMTHF. Furthermore, thiophene-3-nitriles **3a-c** were converted to thiophene-3-carboxmidoximes **4a-c** via reaction with hydroxyl amine. Finally, carboximidamides **4a-c** were cyclized into oxadiazoles **5–19** by reaction with different aryl acid chlorides. The cytotoxicity results regarding MCF-7 cells show that, carboximidamide **4c** and oxadiazoles **9**, **12** and **14** show IC_{50} in sub-micmolar concentration and more potent by 2.3-, 4-, 2.5-, and 10 -fold than PG. Meanwhile, molecules **4c**, **12,** and **14** exhibited higher cytotoxic activity by 5 -, 1.8-, and 2.4- fold, respectively than control on HCT-116 cells. The anti-proliferative activity of tested molecules is correlated to topoisomerase enzyme inhibition, where carboximidamide **4c** and oxadiazoles **9** and **14 were** potent enzyme inhibitors by 2-, 2 -, and 2.7 -fold, respectively than PG. Moreover, the cell cycle flow cytometry analysis indicated that compounds **4c, 9, 11,** and **14** induce cell cycle arrest at G_1 phase of MCF-7 cells. In addition, molecule **14** is stronger apoptotic inducer than PG, as demonstrated by the results of Annexin assay. ELISA measurements for p53 and cell death modulators (Puma, Bax and Bcl-2) show that carboximidamide **4c** and oxadiazoles **9, 12,** and **14** induce upregulation of p53 and increased Puma, and Bax/Bcl-2 ratio levels. The results of the green fluorescence assay exhibited that carboximidamide **4c** and oxadiazoles **9**, **11,** and **14** trigger apoptosis induction via increase active caspase 3/7 percentage. Finally, carboximidamide **4c** and oxadiazole **14** represent promising antitumor and apoptotic agents.

4. Experimental

4.1. Chemistry

4.1.1. General

Melting points of the synthesized molecules are measured with a Stuart melting point apparatus and are uncorrected. The NMR spectra of molecules are measured by Varian Gemini-300BB 400 MHz FT-NMR spectrometers (Varian Inc., Palo Alto, CA). ^1H and ^{13}C spectra are run at 400 and 100 MHz, respectively, in deuterateddimethylsulphoxide (DMSO-d_6). IR spectra of molecules are recorded with a Bruker FT-IR spectrophotometer. Electron impact (EI) mass spectra of molecules are measured on Hewlett Packard 5988 spectrometer. The analysis of elements is carried out at The Regional Center for Mycology and Biotechnology, Al-Azhar University, Egypt. Reactions progresses monitored by thin layer chromatography (TLC) on silica gel precoated plates. The solvent system used for TLC is hexane–ethyl acetate (8.5: 1.5 ml) mixture and the appeared spots are visualized by UV lamp. Silica gel (200–300) mesh is used for Column chromatography. Unless otherwise noted, all solvents and reagents are commercially available and used without further purification. The M.W. work synthesis workstation is Sieno-Mass-II microwave (M.W.) with the specification (2.45GMHz, 1000 W).

4.1.2. Synthesis of 2-amino-thiophene-3-carbonitriles *2a-c*

starting materials **2a-c** were prepared via Gewald three component reaction using *n*-butanol as high boiling solvent instead of ethanol, in brief, a mixture of appropriate ketones **1a-c** (20.0 mmol), propane dinitrile (3.39 g, 30.0 mmol), and sulfur (3.2 g 10.0 mmol) in *n*-butanol (15 ml) was stirred and morpholine (2.61 g, 30.0 mmol) was added dropwise at room temperature with cooling in ice bath. After that, the mixture was irradiated at 150 °C for 10 min in a M.W. reactor. The mixture was cool to room temperature and diluted with petroleum ether (20 ml). The formed brown precipitate is crystallized from ethanol and afford thiophenes **2a-c**. The structure of 2-aminothiophenes **2a-c** was confirmed by their reported physical and spectral data **2a** [24], **2b** [23] and **2c** [25].

4.1.3. Synthesis of 2-(1H-pyrrol-1-yl) thiophene-3-carbonitriles *3a-c*

A mixture of dimethoxytetrahydrofuran (DMTHF) (0.82 g, 6.2 mmol) and glacial acetic (3 ml) was stirred for 5 min at room temperature, followed by the addition of thiophene-3-carbonitriles **2a-c** (0.62 mmol). The reaction mixture was irradiated at 100 °C for 15 min in the M.W. reactor. After cooling, the mixture is diluted with H_2O (20 ml) and the precipitate formed is crystallized from ethanol to furnish thiophenes **3a-c**.

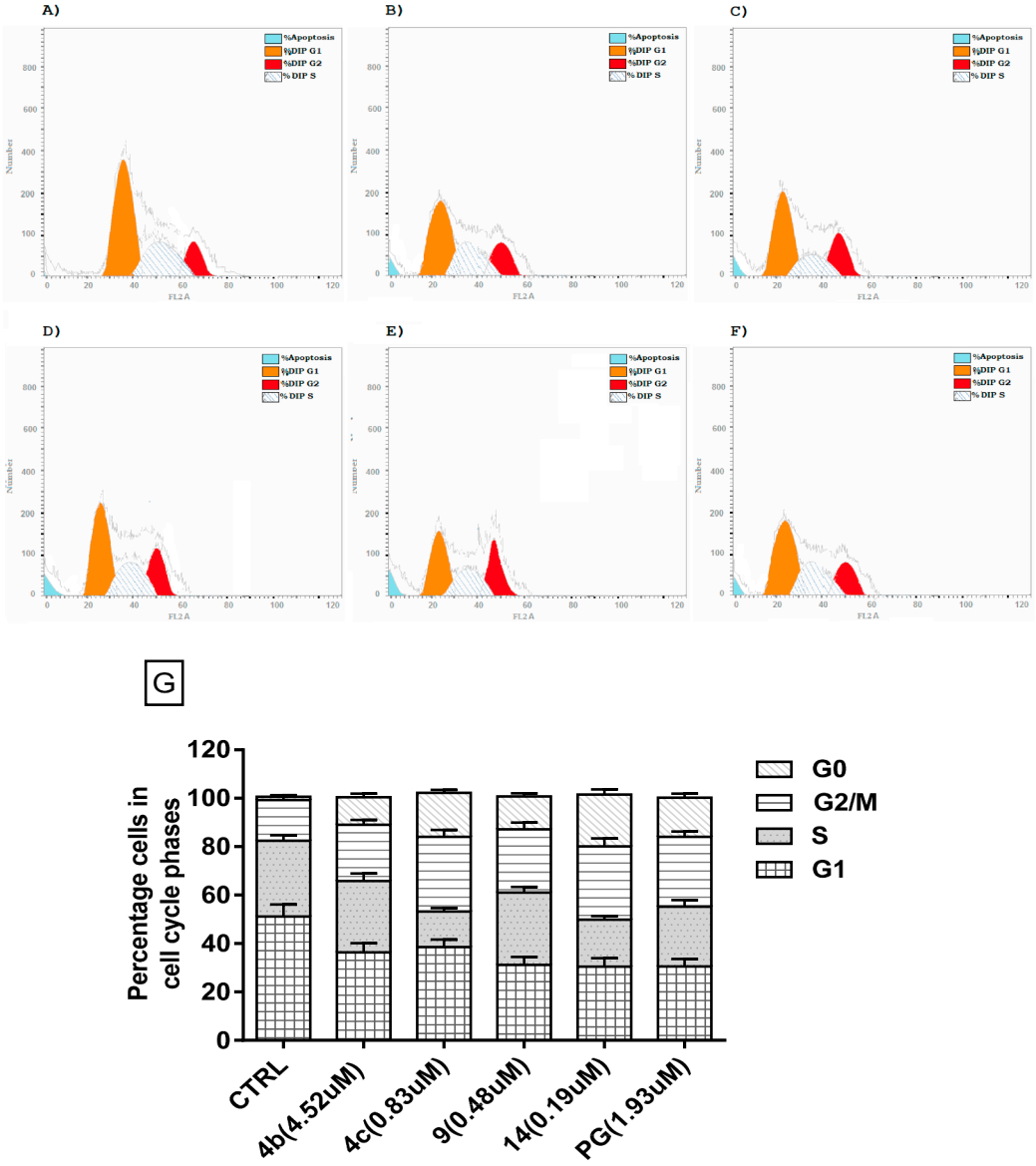

Fig. 7. DNA Flow cytometric analysis of the effect of molecule **4b**, **4c**, **9** and **14** at their IC_{50} on MCF-7 cells for 24 h compared with PG, (A) Control cells, (B) Cells treated with of SSM **4b** (4.52 µM), (C) Cells treated with **4c** (0.83 µM), (D) cells treated with **9** (0.48 µM), (E) Cells treated with **14** (0.19 µM), (F) Cells treated with PG (1.93 µM). (G) Statically analysis of the obtained data and are expressed as mean (n: 3 experiments) ± SEM and statistical comparisons are carried out using one-way analysis of variance (ANOVA) followed by Tukey multiple comparisons.

4.1.3.1. 4, 5-Dimethyl-2-(1H-pyrrol-1-yl) thiophene-3-carbonitrile ***(3a)***. Yield: 0.9 g (74%) White crystal; m.p. 50–53 °C. ^{1}HNMR (DMSO-d_6), δ:2.24 (s, 3H, CH_3), 2.27 (s, 3H, CH_3), 6.27–6.49 (t, 2H, ArH), 6.52–6.59 (d, 2H, 8.7 Hz, ArH) ppm. ^{13}C NMR (DMSO-d_6), δ: 9.9, 12.1, 84.6, 108.4, 115.4, 116.0, 123.2, 135.0, 158.7. IR (KBr, ν cm^{-1}): 2984–2896 (aliph.CH), 2215 (CN). Anal.Calcd. for $C_{11}H_{10}N_2S$ (202.28): C, 65.32; H, 4.98; N, 13.85; Found: C, 65.29; H, 4.84; N, 13.72.

4.1.3.2. 2-(1H-Pyrrol-1-yl)-4, 5, 6, 7-tetrahydrbenzo[b]thiopthene-3-carbonitrile ***(3b)***. Yield: 1.1 g (81%) White crystal; m.p. 73–76 °C (lit,63–65 °C) [24]. ^{1}HNMR (300 MHz, DMSO-d_6), δ: 1.73–1.79 (m, 4H, $2CH_2$), 2.65–2.69 (m, 4H, $2CH_2$), 6.18–6.19 (m, 2H, ArH), 6.91–6.92 (m, 2H, ArH) ppm. ^{13}C NMR (DMSO-d_6), δ: 20.4, 22.9, 23.4, 24.5, 84.0, 108.5, 115.3, 123.2, 134.5, 141.0, 158.1.

4.1.3.3. 3-(4-Methoxyphenyl)-2-(1H-pyrrol-1-yl) thiophene-3-carbonitrile ***(3c)***. Yield: 1.2 g (76%), White crystal; m.p. 122–123 °C. ^{1}H NMR (DMSO-d_6), δ: 3.71(s, 3H, CH_3), 6.40–6.50(m, 3H, ArH), 6.91–7.05 (m, 4H, ArH), 7.32–7.45 (m, 2H, ArH) ppm. ^{13}C NMR (DMSO-d_6), δ: 56.40, 82.3, 108.5, 115.9, 117.9, 123.7, 124.3, 127.8, 128.0, 129.4, 141.2, 160.2. IR (KBr, ν cm^{-1}): 3023 (arom.CH), 2983–2892 (aliph.CH), 2218(CN); Anal.Calcd. for $C_{16}H_{12}N_2OS$ (280.34): C, 68.55; H, 4.31; N, 9.99; Found: C, 68.29; H, 4.64; N, 10.12.

4.1.4. N-hydroxy-2-(1H-pyrrol-1-yl) thiopthene-3-carboximidamides ***4a-c***

Thiophene 3-carbonitrile derivatives **3a-c** (8 mmol) were dissolved in *n*-butanol (15 ml) and treated with Cs CO_3 (5.2 g, 16 mmol) and hydroxyl amine hydrochloride (1.0 g, 14.8 mmol) with stirring for 5 min at room temperature. The reaction mixture was irradiated at 140 °C for 20 min in M.W. reactor. After cooling to room temperature, the mixture was diluted with diethyl ether (20 ml) and the precipitate formed is collected by filtration, washed with ethanol, and dried under vacuum to give carboximidamides **4a-c**.

4.1.4.1. N-Hydroxy-4, 5-dimethyl-2-(1H-pyrrol-1-yl) thiopthene-3-carboximidamide ***(4a)***. Yield: 1.1 g (59%) brown solid; m.p.

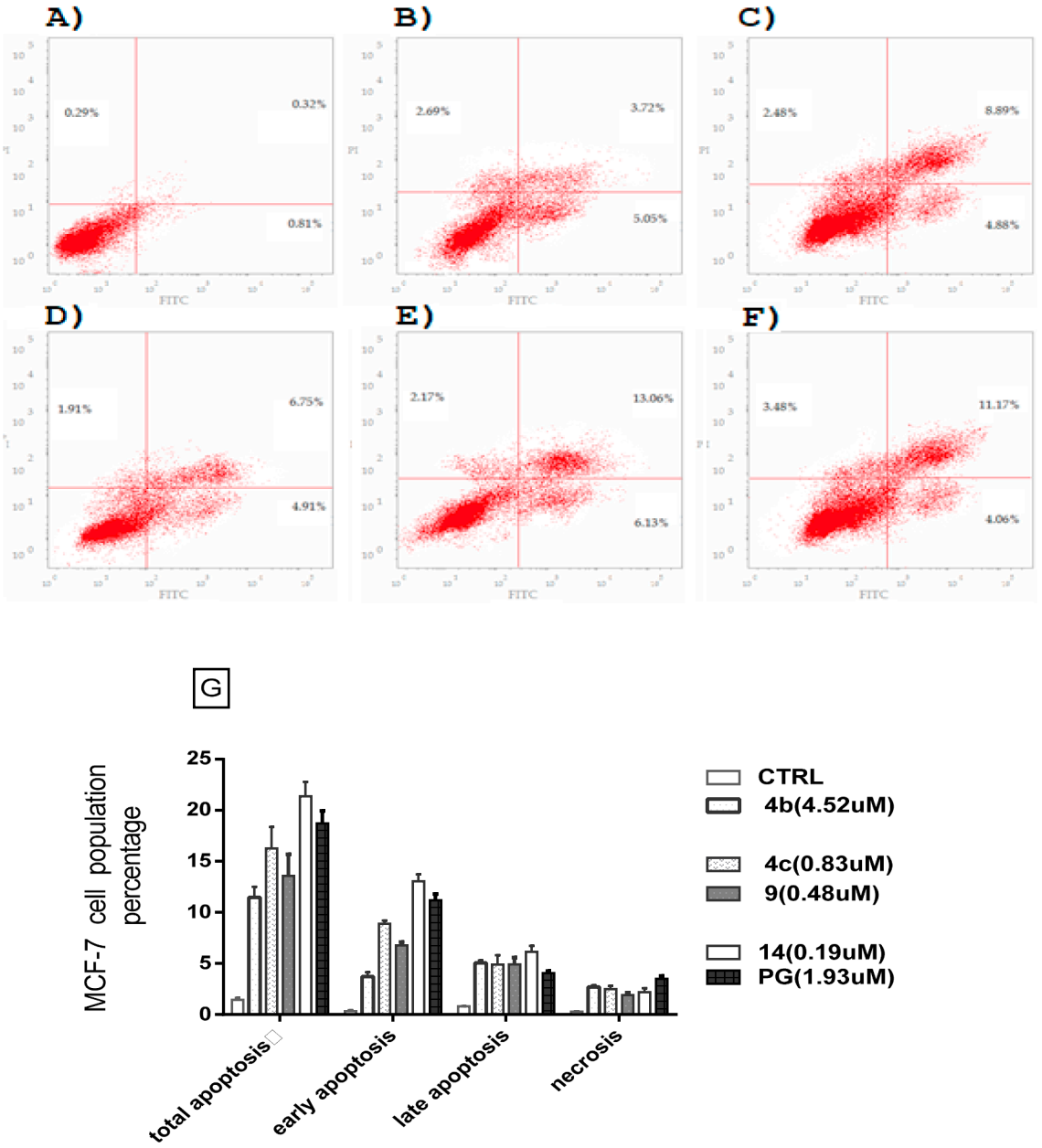

Fig. 8. Annexin V/PI analysis by flow cytometry of MCF-7 cells treated with SSMs **4b**, **4c**, **9** and **14** at their IC_{50} compared with PG as e control for 24 h. (A) Control cells, (B) Cells treated with of SSM **4b** (4.52 μM), (C) Cells treated with **4c** (0.83 μM), (D) cells treated with **9** (0.48 μM), (E) Cells treated with **14** (0.19 μM), (F) Cells treated with PG (1.93 μM). (G) Statistical analysis, data are expressed as mean (n: 3) ± SEM and statistical comparisons are carried out using one-way analysis of variance (ANOVA) followed by Tukey multiple comparisons. The red color represents the stained Annexin V cells.

250–253 °C. ^{1}H NMR (DMSO-d_6), δ: 2.25 (s, 3H, CH_3), 2.31 (s, 3H, CH_3), 4.95 (s, 1H, D_2O exchangeable), 6.23–6.38 (m, 1H, ArH), 6.44–6.49 (d, 1H, 8.7 Hz, ArH), 6.95–6.97 (d, 2H,ArH), 10.63 (s,1H, D_2O exchangeable), 10.73 (s,1H, D_2O exchangeable) ppm. ^{13}CNMR (DMSO-d_6), δ: 10.4, 10.9, 108.3, 120.7, 123.0, 131.5, 134.0, 136.0, 163.2. IR (KBr, ν cm^{-1}): 3412–3090 (NH & OH), 3054 (arom.CH), 2983–2891 (aliph.CH). Anal.Calcd. for $C_{11}H_{13}N_3OS$ (235.31): C, 56.15; H, 5.57; N, 17.86; Found: C, 56.28; H, 5.71; N, 17.61.

*4.1.4.2. N-Hydroxy-2-(1H-pyrrol-1-yl)-4, 5, 6, 7-tetrahydrobenzo[b] thiopthene-3-carboximidamide (**4b**).* Yield: 1.40 g (67%), yellow solid; m.p. 262–265 °C. ^{1}H NMR (DMSO-d_6), δ: 1.60–1.78 (m, 4H, $2CH_2$), 2.72–2.79, (m, 4H, $2CH_2$), 4.90 (s, 2H, D_2O exchangeable), 6.14–6.27 (m, 2H, ArH), 6.91–6.97(m, 2H, ArH), 10.77 (s, 1H, D_2O exchangeable) ppm.; ^{13}C NMR (DMSO-d_6), δ: 20.4, 23.4, 24.5, 24.6, 108.3, 119.6, 123.1, 127.7, 135.6, 137.4, 163.2. IR (KBr, ν cm^{-1}): 3413–3110 (–NH &OH), 3054 (arom.CH), 2984–2890 (aliph.CH). Anal.Calcd. for $C_{13}H_{15}N_3OS$ (261.09): C, 59.74; H, 5.79; N, 16.08; Found: C, 59.82.; H, 0.93; N, 16.11.

*4.1.4.3. N-Hydroxy-4-(4-methoxyphenyl)-2-(1H-pyrrol-1-yl) thiopthene-3-carboximidamide (**4c**).* Yield: 1.45 g (58%), yellow solid; m.p. 286–289 °C. ^{1}H NMR (300 MHz, DMSO), δ: 3.86 (s, 3H, CH_3), 4.92 (s, 2H, D_2O exchangeable), 6.19–6.24 (m, 2H, ArH), 6.34–6.46 (m, 1H, ArH), 6.80–6.85 (s, 2H, ArH), 6.91–7.07 (s, 2H, ArH), 7.39–7.47 (m, 2H, ArH), 10.76 (s, 1H, D_2O exchangeable) ppm. ^{13}CNMR (DMSO-d_6), δ: 56.4, 108.2, 114.8, 118.3, 123.1, 123.3, 127.0, 128.5, 137.4, 138.2, 160.6, 163.4. IR (KBr, ν cm^{-1}): 3373–3041 (–NH &OH), 3054 (arom.CH), 2997–2983 (aliph.CH). Anal.Calcd. for $C_{16}H_{15}N_3O_2S$ (313.37): C, 61.32; H, 4.82; N, 13.41; Found: C, 61.86; H, 4.94; N, 13.33.

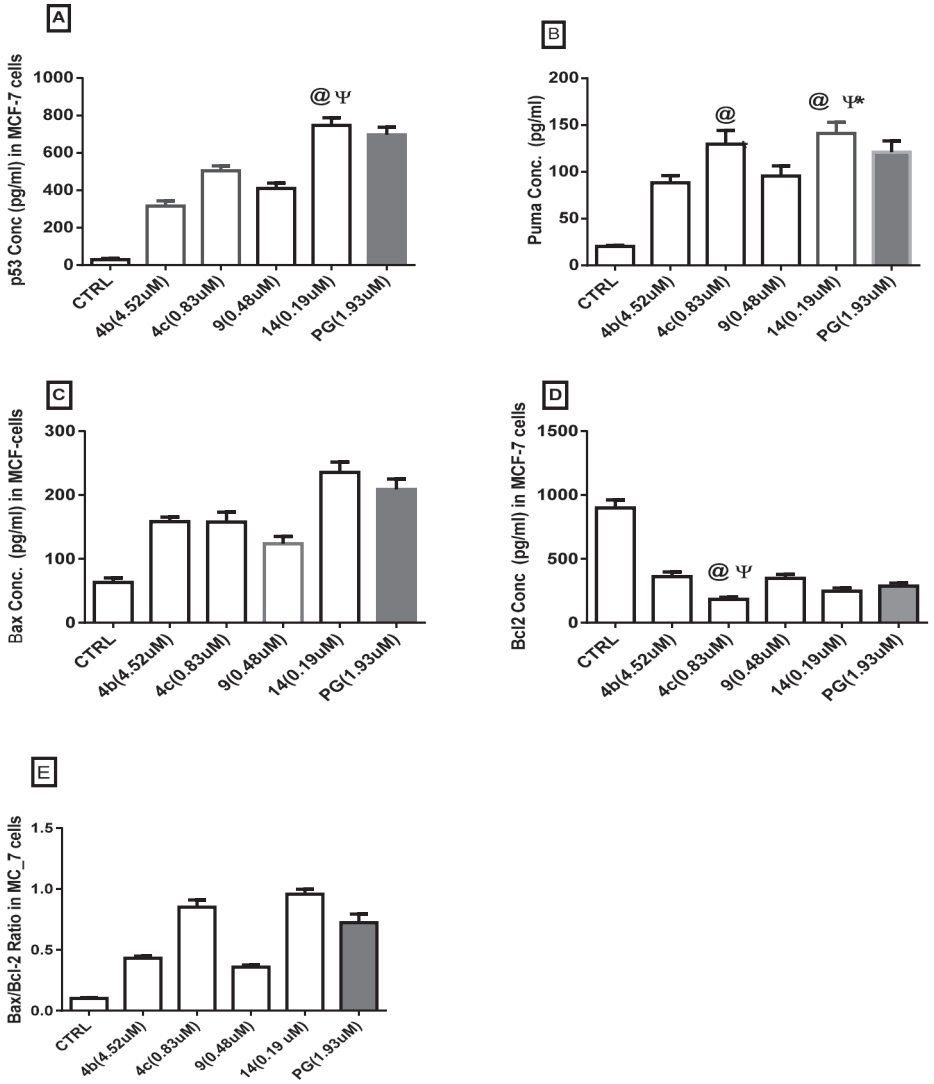

Fig. 9. ELISA-immunoassay for MCF-7 cells treated with SSMs **4b, 4c, 9** and **14** at their IC_{50} compared with untreated cells and PG as positive control and untreated cells for 24 h to measure the concentration of the following proteins, (A) P53, (B) puma, (C) Bax, (D) Bcl-2, (E) Bax/bcl-2 ratio. Data are expressed as mean (n: 3) ± SEM and statistical comparisons are carried out using one-way analysis of variance (ANOVA) followed by Tukey multiple comparisons at $p < 0.05$ where Ψ as significant from CTRL, and @ as significant from PG.

*4.1.5. Synthesis of 5-aryl-3-(2-(1H-pyrrol-1-yl)-thiophen-3-yl)-1, 2, 4-oxadiazoles **5–19***

Thiophene-3-carboximidoximes **4a-c** (0.8 mmol) were dissolved in ethylene glycol (10 ml), then the appropriate acid chloride (0.8 mmol) was added dropwise with cooling and the reaction mixture was stirred at room temperature for 2 min. The reaction mixture was irradiated at 200 °C for 5 min. After cooling, the mixture was diluted with a saturated aqueous $NaHCO_3$ solution (10 ml) and extracted with ethyl acetate (3 × 15 ml). The combined organic layers were dried over Na_2SO_4 and evaporated under reduced pressure. The obtained residue was purified by flash chromatography using a mixture of ethyl acetate:pet. ether (1:9) to give oxadiazoles **5–19**.

*4.1.5.1. 3-[4, 5-Dimethyl-2-(1H-pyrrol-1-yl) thiophen-3-yl]-5-phenyl-1, 2, 4-oxadiazole (**5**)*. Yield: 0.19 g (75%), yellow powder; m.p. 98–100 °C. ^{1}HNMR(DMSO-d_6), δ: 2.23 (s, 3H, CH_3), 2.33 (s, 3H, CH_3), 6.31–6.46 (m, 2H, ArH), 6.50–6.61 (m, 3H, ArH), 6.65–7.28 (m, 2H, ArH), 7.29–7.39 (m, 2H, Ar H) ppm. ^{13}C NMR (DMSO-d_6), δ: 11.1, 13.2, 110.4, 117.3, 124.0, 124.2, 127.5, 128.7, 129.2, 131.7, 134.7, 139.4, 143.5, 166.5, 176.9 ppm. IR (KBr, ν cm^{-1}): 3021 (arom.CH), 2993–2981 (aliph.CH). MS (*m/z*, %): 321.06 (M^+, 15.21), 315.19 (100). Anal.Calcd. for $C_{18}H_{15}N_3OS$ (321.4): C, 67.27; H, 4.70; N, 13.07; Found: C, 67.28; H, 4.74; N, 13.31.

*4.1.5.2. 5-(4-Chlorophenyl)-3-[4, 5-dimethyl-2-(1H-pyrrol-1-yl)thiophen-3-yl]-1, 2, 4-oxadiazole (**6**)*. Yield: 0.16 g (55%), brown powder. m.p. 153–157 °C; ^{1}H NMR (DMSO-d_6), δ: 2.28 (s, 3H, CH_3), 2.31 (s, 3H, CH_3), 6.54 (s, 2H, ArH), 7.05–7.08 (d, 2H, ArH), 7.38–7.40 (d, 2H, ArH), 7.73 (s, 2H, ArH) ppm. ^{13}C NMR (DMSO-d_6) δ: 11.1, 13.2, 110.4, 124.0, 124.2, 127.5, 128.7, 129.2, 131.7, 134.7, 139.5, 143.5, 166.4, 176.9 ppm. IR (KBr,νcm^{-1}): 3021 (arom.CH), 2997–2979 (aliph.CH). MS (*m/z*, %): 355.22 (M^+, 10.25), 331.32 (100). Anal.Calcd. for $C_{18}H_{14}ClN_3OS$ (355.84): C, 60.76; H, 3.97; N, 11.81; Found: C, 60.70; H, 3.84; N, 11.71.

*4.1.5.3. 5-(4-Bromophenyl)-3-[4, 5-dimethyl-2-(1H-pyrrol-1-yl) thiophen-3-yl]1, 2, 4-oxadiazole (**7**)*. Yield: 0.19 g (59%), yellowish white powder. m.p. 132–135 °C. ^{1}H NMR (DMSO-d_6), δ: 2.26 (s, 3H, CH_3), 2.30 (s, 3H, CH_3), 6.55–6.96 (m,4H, ArH), 7.25–7.66 (m, 4H, ArH) ppm. ^{13}C NMR (DMSO-d_6), δ: 11.1, 13.2, 110.4, 124.0, 125.4, 126.4, 127.5, 129.3, 131.7, 134.8, 139.5, 143.5, 166.5, 176.9 ppm. IR (KBr, νcm^{-1}): 3019 (arom.CH), 2995–2980 (aliph.CH). MS (*m/z*, %): 399.12

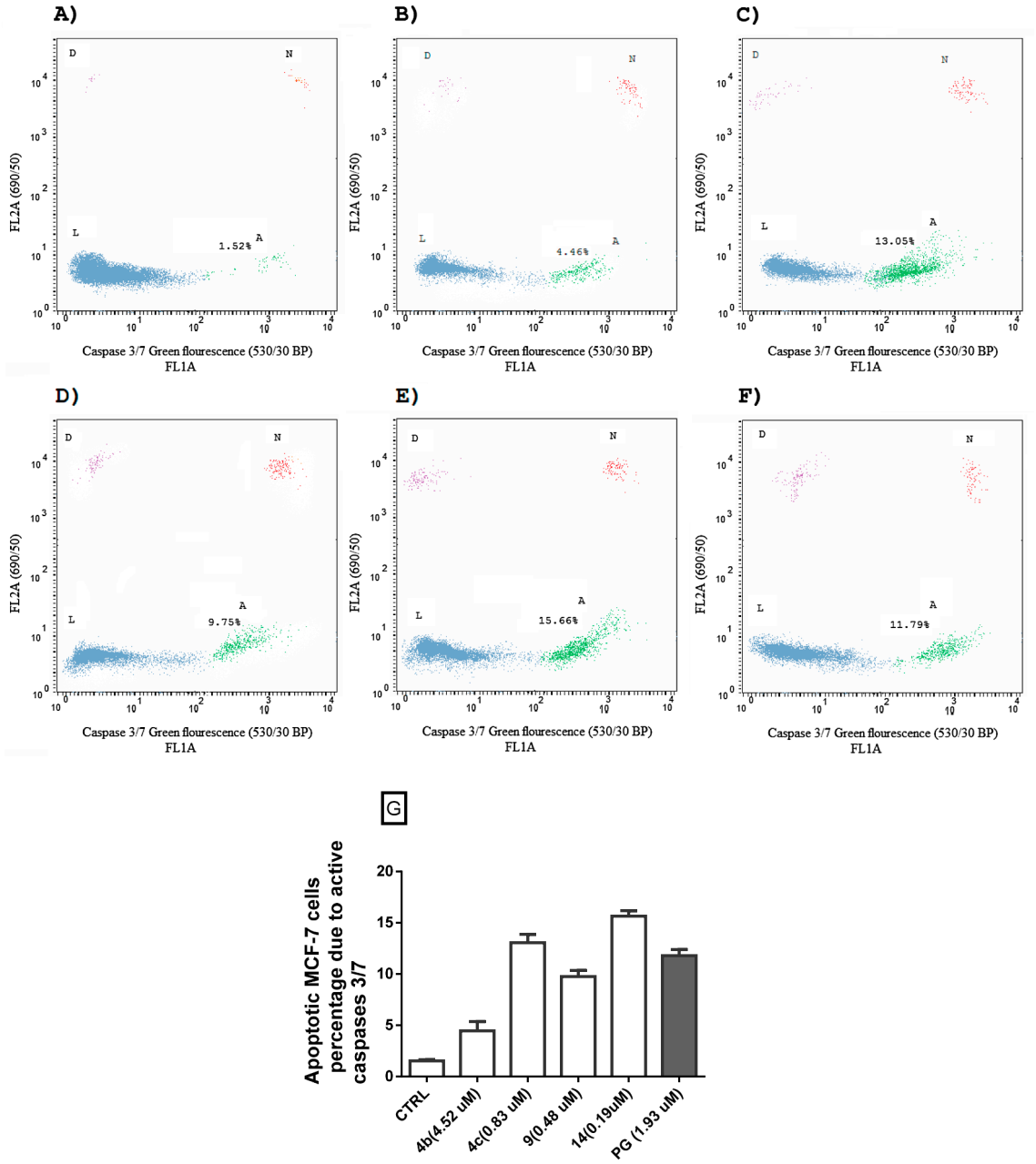

Fig. 10. Annexin V/pacific blue multicolor staining assay for MCF-7 cells after treatment with SSMs **4b**, **4c**, **9**, **14** compared with PG for active caspase 3/7 and apoptosis induction after 24 h. (A) Untreated cells, (B) cells treated with **4b** (4.52 μM), (C) Cells treated with 4c (0.83 μM), (D) Cells treated with **9** (0.48 μM), (E) Cells treated with **14** (0.19 μM), (F) Cells treated with TER (1.93 μM). L: live cells (blue), A: apoptotic cells (green), N: necrotic cells (red), D: dead cells. (G) Graphical presentation for comparison of apoptotic MCF-7 cells due to active caspases 3/7 of the tested molecules and PG, Data represented as Mean ± SD of three independent trials.

(M^+, 15.28), 345.51 (100). Anal.Calcd. for $C_{18}H_{14}BrN_3OS$ (400.29): C, 54.01; H, 3.53; N, 10.50, found: C, 54.22; H, 3.61; N, 10,38.

4.1.5.4. 3-[4,5-Dimethyl-2-(1H-pyrrol-1-yl)thiophen-3-yl]-5-(4-tolyl)1, 2, 4-oxadiazole ***(8)***. Yield: 0.13 g (49%), yellow powder; m.p. 88–90 °C. ^{1}H NMR (DMSO-d_6), δ: 2.30 (s, 3H, CH_3), 2.34 (s, 3H, CH_3), 2.40 (s, 3H, CH_3), 6.55–6.89 (m, 4H, ArH), 7.21–6.26 (m, 2H, ArH), 7.54–7.63 (m, 2H, ArH) ppm. ^{13}C NMR (DMSO-d_6) δ: 11.1, 13.2, 22.1, 110.4, 124.0, 124.1, 127.5, 128.7, 129.2, 131.7, 134.7, 139.4, 143.5, 166.5, 175.8 ppm. IR (KBr, νcm^{-1}): 3027 (arom.CH), 2997–2984 (aliph.CH). MS (*m/z*, %): 334.11 (M^+, 35.51), 301.54 (100). Anal.Calcd. for $C_{19}H_{17}N_3OS$ (335.42): C, 68.03; H, 5.11; N, 12.53; Found: C, 68.14; H, 5.23; N, 12.63.

4.1.5.5. 3-[4,5-Dimethyl-2-(1H-pyrrol-1-yl)thiophen-3-yl]-5-(4-methoxyphenyl)-1, 2, 4-oxadiazole ***(9)***. Yield: 0.16 g (56%),yellow powder; m.p. 167–170 °C; ^{1}H NMR (DMSO-d_6), δ: 2.24 (s, 3H, CH_3), 2.38 (s, 3H, CH_3), 3.80 (s, 3H, –OCH_3), 6.33–6.42 (m, 2H, ArH), 6.44–6.60 (m, 1H, ArH), 6.61–6.68 (m, 3H, ArH), 6.82–6.93 (m, 2H, Ar H) ppm, ^{13}C NMR (DMSO-d_6), δ: 11.1, 13.2, 57.4, 110.4, 124.1, 125.2, 126.4, 127.5, 129.2, 131.7, 134.7, 139.4, 143.4, 166.4, 176.8 ppm. IR (KBr, νcm^{-1}): 3020 (arom.CH), 2996–2982 (aliph.CH). MS (*m/z*, %): 351.17 (M^+, 60.22), 315.41 (100). Anal.Calcd. for $C_{19}H_{17}N_3O_2S$ (351.42): C, 64.94; H, 4.88; N, 11.96; Found: C, 64.74; H, 4.68; N, 11.76.

4.1.5.6. 3-[2-(1H-Pyrrol-1-yl)-4, 5, 6, 7-tetrahydrobenzo[b]thiophen-3-yl]-5-phenyl-1, 2, 4-oxadiazole ***(10)***. Yield: 0.22 g (79%), orange

powder; m.p. 141–146 °C.^{1}H NMR (DMSO-d_6), δ: 1.73–1.82 (m, 4H, $2CH_2$), 2.71–2.91 (m, 4H, $2CH_2$), 6.86–7.01 (m, 2H, ArH), 7.13–7.29 (m, 3H, ArH), 7.37–7.53 (m, 4H, ArH) ppm; ^{13}C NMR (DMSO-d_6), δ: 22.3, 22.6, 25.7, 25.9, 115.0, 117.6, 127.0, 128.3, 131.7, 132.3, 133.4, 134.0, 135.7, 145.6, 164.0, 176.6 ppm. IR (KBr, νcm^{-1}): 3015 (arom.CH), 2993–2980 (aliph.CH). MS (*m/z*, %): 347.13 (M^+, 10.58), 151.22 (100). Anal.Calcd. for $C_{20}H_{17}N_3OS$ (347.43): C, 69.14; H, 4.93; N, 12.09; Found: C, 69.34; H, 4.90; N, 12.11.

*4.1.5.7. 3-[2-(1H-Pyrrol-1-yl)-4, 5, 6, 7-tetrahydrobenzo[b]thiophen-3-yl]-5-(4-chloro phenyl)-1, 2, 4-oxadiazole (**11**)*. Yield: 0.19 g (63%), yellow powder; m.p. 152–156 °C. ^{1}H NMR (DMSO-d_6), δ: 1.75–1.80 (m, 4H, $2CH_2$), 2.61–2.91 (m, 4H, $2CH_2$), 6.47–6.52 (m, 1H, ArH), 6.67–6.79 (m, 4H, ArH), 7.30–7.43 (m, 3H, ArH) ppm. ^{13}C NMR (DMSO-d_6): δ: 22.5, 22.7, 25.8, 26.0, 111.2, 122.3, 123.1, 124.2, 125.1, 127.3, 128.1, 129.3, 140.3, 142.4, 166.7, 176.8 ppm. IR (KBr, νcm^{-1}): 3034 (arom.CH), 2997–2981 (aliph.CH). MS (*m/z*, %): 381.16 (M^+, 10.83), 187.32 (100). Anal.Calcd. for $C_{20}H_{16}ClN_3OS$ (381.88): C, 62.90; H, 4.22; N, 11.00; Found: C, 62.80; H, 4.04; N, 10.81.

*4.1.5.8. 3-[2-(1H-Pyrrol-1-yl)-4, 5, 6, 7-tetrahydrobenzo[b]thiophen-3-yl]-5-(4-bromo phenyl)-1, 2,4-oxadiazole (**12**)*. Yield: 0.23 g (66%), red powder; m.p.121–125 °C. ^{1}H NMR (DMSO-d_6), δ: 1.74–1.80 (m, 4H, $2CH_2$), 2.67–2.73 (m, 4H, $2CH_2$), 6.16–6.20 (m, 1H, ArH), 6.38 (s, 3H, ArH), 6.95–6.98 (m, 2H, ArH), 7.24 (s, 1H, ArH), 7.45 (s, 1H, ArH) ppm; ^{13}C NMR (DMSO-d_6): δ: 22.6, 22.8, 25.2, 26.0, 106.0, 121.2, 121.8, 129.5, 130.7, 132.0, 133.7, 134.8, 136.1, 140.0, 166.2, 175.4 ppm. IR (KBr, νcm^{-1}): 3034 (arom.CH), 2994–2983 (aliph.CH). MS (*m/z*, %): 425.44 (M^+, 5.98), 331.61 (100). Anal.Calcd. for $C_{20}H_{16}BrN_3OS$ (426.33): C, 56.34; H, 3.78; N, 9.86; Found: C, 56.44; H, 3.84; N, 9.71.

*4.1.5.9. 3-[2-(1H-Pyrrol-1-yl)-4, 5, 6, 7-tetrahydrobenzo[b]thiophen-3-yl]-5-(4-tolyl)-1, 2, 4-oxadiazole (**13**)*. Yield: 0.17 g (60%), red powder; m.p. 142–146 °C. ^{1}H NMR (DMSO-d_6), δ: 1.76–1.95 (m, 4H, $2CH_2$), 2.15 (s, 3H, CH_3), 2.65–2.91 (m, 4H, $2CH_2$), 6.44–6.60 (m, 2H, ArH), 6.62–6.84 (m, 3H, ArH), 6.99–7.05 (m, 2H, ArH), 7.16–7.46(m, 1H, ArH) ppm. ^{13}C NMR (DMSO-d_6), δ: 21.4, 22.6, 22.8, 25.2, 26.0, 112.2, 121.0, 124.6, 125.8, 128.8, 131.4, 133.5, 138.1, 140.9, 141.0, 167.7, 173.1 ppm. IR (KBr, νcm^{-1}): 3031 (arom.CH), 2995–2980 (aliph.CH). MS (*m/z*, %): 361.21 (M^+, 35.65), 257.51 (100). Anal.Calcd. for $C_{21}H_{19}N_3OS$ (361.46): C, 69.78; H, 5.39; N, 11.63; Found: C, 69.88; H, 5.44; N, 11.71.

*4.1.5.10. 3-[2-(1H-Pyrrol-1-yl)-4, 5, 6, 7-tetrahydrobenzo[b]thiophen-3-yl]-5-(4-methoxyphenyl)-1, 2, 4-oxadiazole (**14**)*. Yield: 0.18 g (58%), buff solid; m.p. 133–137 °C; ^{1}H NMR (DMSO-d_6), δ: 1.74–1.80 (m, 4H, $2CH_2$), 2.60–2.69 (m, 4H, $2CH_2$), 3.84 (s, 3H, –OCH_3), 6.16–6.20 (m, 2H, ArH), 6.21–6.38 (m, 2H, ArH), 6.95–6.98 (m, 2H, ArH), 7.23–7.56 (m, 2H, ArH) ppm. ^{13}C NMR (DMSO-d_6), δ: 22.2, 22.9, 25.4, 25.6, 56.5, 105.9, 112.2, 121.4, 126.0, 128.7, 132.6, 133.6, 135.6, 145.7, 153.1, 166.0, 176.7 ppm. IR (KBr, νcm^{-1}): 3024 (arom.CH), 2990–2982 (aliph.CH). MS (*m/z*, %): 377.12 (M^+, 10.05), 343.56 (100). Anal.Calcd. for $C_{21}H_{19}N_3O_2S$ (377.46): C, 66.82; H, 5.07; N, 11.13; Found: C, 66.77; H, 5.14; N, 11.10.

*4.1.5.11. 5-Phenyl-3-(4-methoxyphenyl-2-(1H-pyrrol-1-yl)thiophen-3-yl)-1, 2, 4-oxadiazole (**15**)*. Yield: 0.23 g (71%), orange powder; m.p. 122–126 °C. ^{1}H NMR (DMSO-d_6), δ: 3.84 (s, 3H, –OCH_3), 6.20–6.34 (m, 2H, ArH), 6.36–6.66 (m, 2H, ArH), 6.70–6.73 (m, 3H, ArH), 6.98–7.08 (m, 3H, ArH), 7.14–7.18 (m, 2H, ArH), 7.53–7.67 (m, 2H, ArH) ppm. ^{13}C NMR (DMSO-d_6): δ: 55.8, 111.7, 112.0, 117.1, 118.7, 119.5, 121.5, 121.6, 122.7, 129.5, 130.7, 132.5, 134.8, 135.9, 136.8, 149.0, 165.9, 176.6 ppm. IR (KBr, νcm^{-1}): 3028 (arom.CH), 2998–2980 (aliph.CH). MS (*m/z*, %): 399.10 (M^+, 39.23), 377.16 (100). Anal.Calcd. for $C_{23}H_{17}N_3O_2S$ (399.46): C, 69.15; H, 4.29; N, 10.52; Found: C, 69.23; H, 4.50; N, 10.71.

*4.1.5.12. 5-(4-Chlorophenyl)-3-[4-(4-methoxyphenyl)-2-(1H-pyrrol-1-yl) thiophen-3-yl)-1, 2, 4-oxadiazole (**16**)*. Yield: 0.20 g (59%), red powder; m.p. 166–170 °C. ^{1}H NMR (DMSO-d_6), δ: 3.82 (s, 3H, OCH_3), 6.26–6.36 (m, 3H, ArH), 6.76–6.79 (m, 4H, ArH), 6.99–7.29 (m, 4H, ArH), 7.32–7.39(m, 2H, ArH) ppm. ^{13}C NMR (DMSO-d_6): ^{13}C NMR (DMSO-d_6), δ: 56.5, 106.0, 112.3, 113.2, 121.2, 129.5, 130.6, 132.0, 132.1, 134.9, 136.8, 140.0, 146.0, 149.0, 153.3, 167.0, 175.4 ppm. IR (KBr, νcm^{-1}): 3031 (arom.CH), 2993–2982 (aliph.CH). MS (*m/z*, %): 433.10 (M^+, 5.25), 367.33 (100). Anal.Calcd. for $C_{23}H_{16}ClN_3O_2S$ (433.91): C, 63.66; H, 3.72; N, 9.68; Found: C, 63.88; H, 3.84; N, 9.71.

*4.1.5.13. 5-(4-Bromophenyl)-3-[4-(4-methoxyphenyl)-2-(1H-pyrrol-1-yl) thiophen-3-yl)-1, 2, 4-oxadiazole (**17**)*. Yield: 0.25 g (65%),brown solid; m.p. 172–173 °C. ^{1}H NMR (DMSO-d_6), δ: 3.81 (s, 3H, –OCH_3), 6.20–6.21 (m, 2H, ArH), 6.53–6.56 (m, 2H, ArH), 6.88–7.09 (m, 5H, ArH), 7.21–7.23 (m, 2H, ArH), 7.40–7.42 (m, 2H, ArH)ppm. ^{13}C NMR (DMSO-d_6), δ: 56.2, 105.4, 106.2, 107.2, 112.3, 113.0, 118.3, 122.0, 127.9, 128.0, 129.4, 132.2, 135.0, 139.8, 146.0, 165.4, 176.8 ppm. IR (KBr, νcm^{-1}): 3028 (arom.CH), 2992–2980 (aliph.CH). MS (*m/z*, %): 477.12 (M^+, 35.21), 413.23 (100). Anal.Calcd. for $C_{23}H_{16}BrN_3O_2S$ (478.36): C, 57.75; H, 3.37; N, 8.78; Found: C, 57.65; H, 3.30; N, 8.70.

*4.1.5.14. 5-(4-Methylphenyl)-3-[4-(4-methoxyphenyl)-2-(1H-pyrrol-1-yl) thiophen-3-yl]-1, 2, 4-oxadiazole (**18**)*. Yield: 0.19 g (58%), yellowish white powder; m.p. 152–156 °C. ^{1}H NMR (DMSO-d_6): δ: 2.38 (s, 3H, CH_3), 3.78 (s, 3H, –OCH_3), 6.33–6.36 (m, 3H, ArH), 6.68–6.94 (m, 2H, ArH), 7.05–7.18(m, 3H, ArH), 7.20–7.44 (m, 3H, ArH), 7.55(s, 1H, ArH, 7.58 (s, 1H, ArH). ^{13}C NMR (DMSO-d_6), δ: 20.6, 56.6, 106.0, 117.7, 120.0, 124.6, 127.0, 128.6, 133.6, 135.7, 139.1, 141.1, 142.5, 145.6, 153.2, 153.7, 167.7, 174.7 ppm. IR (KBr, νcm^{-1}): 3012 (arom.CH), 2996–2987 (aliph.CH). MS (*m/z*, %): 413.11 (M^+, 25.22), 347.16 (100). Anal.Calcd. for $C_{24}H_{19}N_3O_2S$ (413.49): C, 69.71; H, 4.63; N, 10.16; Found: C, 69.88; H, 4.44; N, 10.17.

*4.1.5.15. 5-(4-Methoxyphenyl)-3-(4-methoxyphenyl-2-(1H-pyrrol-1-yl) thiophen-3-yl)-1, 2, 4-oxadiazole (**19**)*. Yield: 0.16 g (46%), red powder; m.p. 190–193 °C. ^{1}H NMR (DMSO-d_6), δ: 3.67 (s, 3H, –OCH_3), 3.78 (s, 3H, –OCH_3), 6.26–6.38 (m, 4H, ArH), 6.41–6.53 (m, 3H, ArH), 6.56–6.95 (m, 3H, ArH), 7.07–7.55 (m, 3H, ArH). IR (KBr, νcm^{-1}): 3022 (arom.CH), 2991–2976 (aliph.CH). MS (*m/z*, %): 429.46 (M^+, 10.21), 347 (100). Anal.Calcd. for $C_{24}H_{19}N_3O_3S$ (429.49): C, 67.12; H, 4.46; N, 9.78; Found: C, 67.34; H, 4.74; N, 9.71.

4.2. In vitro antiproliferative studies

4.2.1. In vitro cell growth inhibition

4.2.1.1. Materials. The human breast adenocarcinoma (MCF-7) and colorectal cancer (HCT-116) cell lines were obtained from american type culture collection. Prodigiosin as positive control and all other chemicals and reagents were purchased from Sigma or Invitrogen.

4.2.1.2. Methodology of MTT assay. The cells are grown on RPMI-1640 medium supplemented with 10% inactivated fetal calf serum and 50 μg/ml gentamycin. The cells were maintained at 37 °C in a humidified atmosphere with 5% CO_2 and are subculture two to three times a week. For antitumor assays, the MCF-7 cells were suspended in medium at concentration 5×10^4 cell/well in Corning® 96-well tissue culture plates and then incubated for 24 h. The tested molecules **3a-c**, **4a-c, 5–19** and PG were then added into 96-well plates to achieve six concentrations for each molecule (50, 20, 10, 1.0, 0.1, 0.001 μM), respectively. Six vehicle controls with media or 0.5% DMSO are run for each 96 well plate as a control. After incubating for 24 h, the numbers

of viable cells were determined by the tetrazolium MTT (3-(4, 5-dimethylthiazolyl-2)-2, 5-diphenyltetrazolium bromide) assay [33]. Briefly, the media was removed from the 96 well plate and replaced with 100 µl of fresh culture RPMI 1640 medium without phenol red then 10 µl of the 12 mM MTT stock solution (5 mg of MTT in 1 ml of PBS) to each well including the untreated controls. The 96 well plates were then incubated at 37 °C and 5% CO_2 for 4 h. An 85 µl aliquot of the media is removed from the wells, and 50 µl of DMSO is added to each well and mixed thoroughly with the pipette and incubated at 37 °C for 10 min. Then, the optical density is measured at 590 nm with the microplate reader (Sun Rise, TECAN, Inc, USA) to determine the number of viable cells. The relation between surviving cells and drug concentration was plotted to get the survival curve of each tumor cell line after treatment with the specified compound. The 50% inhibitory concentration (IC_{50}), the concentration required to cause toxic effects in 50% of intact cells, was estimated from graphic plots of the dose response curve for each concentration using Graph Pad Prism software. The experiment is repeated three times.

4.2.2. In vitro topoisomerase 2 enzymes assay

4.2.2.1. Materials. The *in vitro* enzyme inhibition determination for the synthesized molecule tested is carried out in BPS Bioscience Corporation, San Diego, CA, USA (www.bpsbioscience.com). The following served as the enzyme sources, Poly (Glu, Tyr) sodium salt (4:1, Glu:Tyr) (Sigma#P7244) served as the standardized substrate & Kinase-Glo Plus Luminescence kinase assay kit (Promega # V3772) is used. The assay is performed using Kinase-Glo Plus luminescence kinase assay kit (Promega).

4.2.2.2. Methodology. The tested molecules **4b**, **4c**, **9**, **11**, **12**, **14** and PG were diluted to 100 µl in 10% DMSO and 5 µl of the dilution is added to a 50 µl reaction so that the final concentration of DMSO is 1% in all of reactions. All of the enzymatic reactions were conducted at 30 °C for 40 min. The 50 µl reaction mixture contains 40 mM Tris, pH 7.4, 10 mM $MgCl_2$, 0.1 mg/ml BSA, 1 mM DTT (Dithiothreitol), 10 µM ATP, enzyme substrate and respective kinases. After the enzymatic reaction, 50 µl of enzyme-Glo Plus luminescence topoisomerase assay solution (Promega) was added to each reaction and the plate is incubated for 5 min at room temperature. Luminescence signal was measured using a BioTek Synergy 2 microplate reader. The luminescence data were analyzed using the computer software, Graphpad Prism. The difference between luminescence intensities in the abscence of topoIIβ (Lu_t) and in the prescence of topo IIβ (Lu_c) is defined as 100% activity (Lu_t-Lu_c). The values of topo IIβ activity percentages versus a series of tested molecules concentrations (1 nM, 10 nM, 100 nM, 1 µM, 10 µM) are then plotted using non-linear regression analysis of sigmoidal dose-response curve generated with the equation: $Y: B + (T\text{-}B)/1 + 10^{((\log EC50\text{-}X) \times Hill\ Slope)}$, where Y: percent activity, B: minimum percent activity, T: maximum percent activity, X: logarithm of compound and Hill Slope: slope factor or Hill coefficient. The IC_{50} value was determined by the concentration causing a half-maximal percent activity using Graph pad Prism software. The experiment is repeated three times.

4.2.3. In vitro DNA immunofluorescence binding assay

Histochemical immunofluorescence assay for establishing indirect DNA binding affinity is performed [34]. Briefly, slides of fixed MCF-7 cells were rinsed in three changes of PBS. Non-specific binding is prevented by incubation in blocking solution (10% fetal bovine serum in PBS) at 37 °C for 30 min. Slides were incubated for 30 min at 37 °C with pico-green dye solution (Abcam Inc., USA). Slides were rinsed again with PBS to remove excess dye, then treated with ethanolic solution of the tested compounds **4b**, **9, 11**, **14** and PG at concentration of their IC_{50} at 37 °C for 24 h. After washing, images were visualized at 642–645 nm using a fluorescence microscope (Axiostar Plus, Zeiss, Goettingen, Germany) equipped with image analyzer and digital camera (Power Shot A20, Canon, USA). The experiment is repeated three times.

4.2.4. In vitro cell cycle DNA flow cytometry analysis

The MCF-7 cells (3×10^6 cells/mL) are seeded in RPMI-1640 medium in T-75 flasks for 24 h and then treated with tested molecules **4b**, **9, 11**, **14** and PG at their IC_{50} (µM) for 24 h. The MCF-7 cells were then collected by trypsinization, wash with PBS and fix in ice-cold absolute alcohol. After that, cells were stained using the cycle test™ Plus DNA Reagent Kit (BD Biosciences, San Jose, CA, USA) according to the manufacturer's instructions [35]. Cell cycle distribution was calculated using CELLQUEST software (Becton Dickinson Immuno-cytometry Systems, San Jose, CA, USA). The experiment is repeated three times.

4.2.5. In vitro Annexin-V/PI staining analysis

The MCF-7 (1×10^6) cells are seeded to a plate and cultured for 24 h, after which indicated dose of tested molecules **4b**, **9, 11**, **14** and PG were added and incubated for up 24 h. Cells were then washed with PBS and detached by trypsin followed by neutralization with culture medium. The detached cells were collected into a 15-mL centrifuged tube, wash with ice-cold PBS twice, and centrifuge at 1200 rpm for 5 min to remove supernatant. A volume of 0.1 ml binding buffer, was added to the MCF-7 cells, followed by adding 5 µl of annexin V-FITC and 5 µl of 50 µg/mL PI staining reagents. After mixing homogeneously and reacting at 25 °C for 15 min in the dark, the apoptotic cell population was analyzed by a flow cytometer [FACS Calibur flow cytometer (BD Biosciences)]. The experiment is repeated three times.

4.2.6. In vitro ElISA immunoassay for p53 and cell death modulators

4.2.6.1. Materials. The levels of p53, Puma, Bax, Bcl-2 were measured in MCF-7 cells treated with the molecules **4b**, **4c**, **9**, **11**, **12**, **14** and PG for 24 h using ELISA colorimetric kits. All the procedures were performed according to the manufacturer's instructions, Sigma Puma ELISA Human (RAB0500)· $^{DRG®}$ Human Bax ELISA (EIA-4487) Marburg, Germany. Bcl-2 ELISA Kit Invitrogen Corporation 1600 Faraday Avenue Carlsbad.

4.2.6.2. Methodology. The levels of the anti-apoptotic marker Bcl-2 as well as the p53 and apoptotic markers Puma, Bax, Bcl-2 was measured using ELISA colorimetric kits per the manufacturer's instructions. The optical densities were measured at 450 nm using ROBONIK P2000 SPECTROPHOTOMETER wl 450 nm, reference 630 nm. The intensity of the color is proportional to the amount of the corresponding parameter bound in the initial step. The experiment is repeated three times.

4.2.7. In vitro green flow cytometry assay for active caspase 3/7

The enzymatic activities of caspase 3/7 are measured in cell lysates (100 µg protein in 50 µL lysis buffer) using Cell Event™ Caspase-3/7 Green Flow Cytometry Assay Kit, Catalog Number (C10427) per the manufacturer's instructions. Briefly, control and treated MCF-7 cell (2.5×10^5/mL) with molecules **4b**, **4c**, **9**, **11**, **12**, **14** and PG for 24 h are washed with ice cold PBS, MCF-7 cell lysates are combined with reaction buffer and incubated with specific colorimetric substrates (Caspase 3/7 Detection Reagent) at 37 °C for 6 h. The samples are measured at 488 nm in BD FACS Calibur flow cytometer. The experiment is repeated three times.

Acknowledgments

The author is filled with respect to the memory of Dr. Ibrahim Abouelish, founder of Sekem Corporation for supporting this work. The author also grateful Dr. Esam Rashwan, Head of the confirmatory diagnostic unit VACSERA-EGYPT, for carrying out the cytotoxicity screening and other cell death modulators

References

[1] S. Kumar, M.K. Ahmad, M. Waseem, A.K. Pandey, Drug targets for cancer treatment, Med. chem. 115–123 (2015), https://doi.org/10.4172/2161-0444.1000252.

[2] K. Muthu, Madhavi M. Kathiravan, Aparna S. Khilare, A. Madhuri, Design and development of topoisomerase inhibitors using molecular modelling studies, J. Chem. Biol. 6 (2013) 25–36, https://doi.org/10.1007/s12154-012-0079-9.

[3] S. Hoelder, P.A. Clarke, P. Workman, Discovery of small molecule cancer drugs: successes, challenges and opportunities, Mol. Oncol. 6 (2) (2012) 155–176, https://doi.org/10.1016/j.molonc.2012.02.004.

[4] L.X. Zhao, T.S. Kim, S.H. Ahn, T.H. Kim, E.K. Kim, W.J. Cho, H. Choi, C.S. Lee, J.A. Kim, T.C. Jeong, C. Change, E.S. Lee, Synthesis, topoisomerase I inhibition and antitumor cytotoxicity of terpyridine derivatives, Bioorg. Med. Chem. Lett. 11 (2001) 2659–2662, https://doi.org/10.1016/S0960-894X(01)00531-5.

[5] A. Hassanpour, C.A. De Carufel, S. Bourgault, P. Forgione, Synthesis of 2, 5-diaryl-substituted thiophenes as helical mimetics: towards the modulation of islet amyloid polypeptide (IAPP) amyloid fibril formation and cytotoxicity, Chem. Eur. J. 20 (2014) 2522–2528, https://doi.org/10.1002/chem.201303928.

[6] M. Ismail, R.K. Arafa, M.M. Youssef, W.M. El-Sayed, Anticancer, antioxidant activities and DNA affinity of novel monocationic bithiophenes and analogues, Drug Des Devel Ther. 8 (2014) 1659–1672.

[7] N. Darshan, H.K. Manonmani, Prodigiosin and its potential applications, J. Food Sci. Technol. 52 (9) (2015) 5393–5407, https://doi.org/10.1007/s13197-015-1740-4.

[8] U.H. Preya, K.T. Lee, N.J. Kim, J.Y. Lee, D.S. Jang, J.H. Choi, The natural prodigiosin induces S phase cell cycle arrest of human ovarian cancer cells via the generation of ROS stress, Chem. Biol. Interact. 25 (272) (2017) 72–79, https://doi.org/10.1016/j.cbi.2017.05.011.

[9] H.Z. Zhang, S. Kasibhatla, J. Kuemmerle, Mason K.O. Kemnitzer, L. Qiu , C.C. Grundy, B. Tseng, J. Drewe, S.X. Cai, Discovery and structure-activity relationship of 3-aryl-5-aryl-1, 2, 4-oxadiazolesas a new series of apoptosis inducers and potential anticancer agents, J. Med. Chem., 11; 48(16) (2005) 5215–5223. http://doi.org/10.1055/s-0030-1260035.

[10] Y. Arthur, Meredith C. Shaw, Flynn G. Henderson, B. Samulitis, H. Han, P. Steve, H.H. Stratton, S. Chow, Laurence H. Hurley, T.D. Robert, Characterization of novel diaryl oxazole-based compounds as potential agents to treat pancreatic cancer, J. Pharmacol. Exp. Therap. 331 (2009) 636–647, https://doi.org/10.1124/jpet.109.156406.

[11] I. Reines, M. Kietzmann, R. Mischke, T. Schering, A. Lu, B. Kleuser, W. Baumer, Topical application of sphingosine-1-phosphate and FTY720 attenuate allergic contact dermatitis reaction through Inhibition of dendritic cell migration, J. Invest. Dermatol 129 (2009) 1954–1962, https://doi.org/10.1038/jid.2008.454.

[12] D. Simoni, M. Roberti, F.P. Invidiata, R. Rondanin, R. Baruchello, C. Malagutti, A. Mazzali, M. Rossi, S. Grimaudo, F. Capone, L. Dusonchet, M. Meli, M.V. Raimondi, M. Landino, N. D'Alessandro, M. Tolomeo, D. Arindam, S. Lu, D.M. Benbrook, Heterocycle-containing retinoids. Discovery of a novel isoxazole possessing potent apoptotic activity in multidrug and drug-induced apoptosis-resistant cells, J. Med. Chem. 44 (2001) 2308–2318, https://doi.org/10.1021/jm0010320.

[13] S. Kovačević, M. Karadžić, S. Podunavac-Kuzmanović, L. Jevrić, Binding affinity toward human prion protein of some anti-prion compounds - assessment based on QSAR modeling, molecular docking and non-parametric ranking, Eur. J. Pharm. Sci. 1 (111) (2018) 215–225, https://doi.org/10.1016/j.ejps.2017.10.004.

[14] M. Taha, N.H. Ismail, S. Imran, E.H. Anour, M. Selvaraj, W. Jamil, M. Ali, S.M. Kashif, F. Rahim, K.M. Khan, M.I. Adenan, Synthesis and molecular modelling studies of phenyl linked oxadiazole-phenylhydrazone hybrids as potent antileishmanial agents, Eur. J. Med. Chem. 126 (2017) 1021–1033, https://doi.org/10.1016/j.ejmech.2016.12.019.

[15] H. Ullah, F. Rahim, M. Taha, I. Uddin, A. Wadood, S.A.A. Shah, R.K. Farooq, M. Nawaz, Z. Wahab, K.M. Khan, Synthesis, molecular docking study and in vitro thymidine phosphorylase inhibitory potential of oxadiazole derivatives, Biorg. Chem. 78 (2018) 58–67, https://doi.org/10.1016/j.bioorg.2018.02.020.

[16] M. Taha, S. Imran, F. Rahim, A. Wadood, K.M. Khan, Oxindole based hybrid analogs; Novel α-glucosidase inhibitors, Bioorg. Chem. 76 (2018) 273–280, https://doi.org/10.1016/j.bioorg.2017.12.001.

[17] M.T. Javid, F. Rahim, M. Taha, M. Nawaz, A. Wadood, M. Ali, A. Mosaddik, S.A.A. Shah, R.K. Farouq, Synthesis, SAR elucidations and molecular docking study of newly designed isatin based oxadiazole analogs as potent inhibitors of thymidine phosphorylase, Bioorg. Chem. 79 (2018) 323–333, https://doi.org/10.1016/j.bioorg.2018.05.011.

[18] M. Taha, U. Rahid, S. Imran, M. Ali, Rational design of bis-indolylmethane-oxadiazole hybrids as inhibitors of thymidine phosphorylase, Bioorg. Med Chem. 26 (2018) 3654–3663, https://doi.org/10.1016/j.bmc.2018.05.046.

[19] J. Boström, A. Hogner, A.L. linàs, E. Wellner, A.T. Plowright, Oxadiazoles in medicinal chemistry, J. Med. Chem. 55 (2012) 1817–1830, https://doi.org/10.1016/j.bmc.2018.05.046.

[20] L. Yang, Mechanisms of apoptosis resistance in breast cancer, Breast Cancer Mol. Med. 841–858 (2006), https://doi.org/10.1007/978-3-540-28266-2_39.

[21] G. Gu, D. Dustin, S.A. Fuqua, Targeted therapy for breast cancer and molecular mechanisms of resistance to treatment, Curr. Opin. Pharmacol. 31 (2016) 97–103, https://doi.org/10.1016/j.coph.2016.11.005.

[22] Suresh C. Ameta, Pinki B. Punjabi, Rakshit Ameta, Chetna Ameta, Microwave-assisted organic synthesis, A Green chemical approach, first edition, 6-8 (2015).

[23] M.M. Mojtahedi, M.A. Saeed, P. Mahmoodi, M. Adib, Convenient synthesis of 2-aminothiophene derivatives by acceleration of Gewald reaction under ultrasonic aqueous conditions, Synthet. Commun. 1 (40) (2010) 2067–2074, https://doi.org/10.1080/00397910903219435.

[24] F. Moeinpour, N. Dorostkar, M. Vafaei, Mg/La Mixed oxide as an efficient heterogeneous basic catalyst for synthesis of 2-aminothiophenes under microwave irradiation, Synthet. Commun. 42 (2012) 2367–2374.

[25] R. Bai, P. Liu, J. Yang, C. Liu, Y. Gu, Facile synthesis of 2-aminothiophenes using $NaAlO_2$ as an eco-effective and recyclable catalyst, ACS Sustain. Chem. Eng. 3 (7) (2015) 1292–1297, https://doi.org/10.1021/sc500763q.

[26] M.S. Abaee, A. Hadizadeh, M.M. Mojtahedi, M.R. Halvagar, Exploring the scope of the Gewald reaction: expansion to a four-component process, Tetrahedron Lett. 58 (2017) 1408–1412.

[27] K.C. Miles, S.M. Mays, B.K. Southerland, T.J. Auvil, D.M. Ketcha, The Clauson-Kaas pyrrole synthesis under microwave irradiation, ARKIVOC 181–190 (2009), http://www.arkat-usa.org/get-file/32751/.

[28] R. Sylvain, Boulouard F. Moult, R. Max, G. Béatrice, D. Michelle, Preparation of pyrrolo[1, 2-a]thieno[3,2- f][1, 4] diazepines as drugs, Eur. Pat. Appl., EP0446133A1 (1991). https://patents.google.com/patent/EP0446133A1/en.

[29] M.M. Badran, S.M.A. Roshdy, Mohammed K. Abd El-Hameid, Synthesis of certain fused pyrrolothieno [3,2-e] pyrazine derivatives with possible anxiolytic activity, OCAIJ 9 (11) (2013) 427–436 https://www.tsijournals.com/articles/synthesis-of-certain-fused-pyrrolothieno3-2e-pyrazine-derivatives-with-possible-anxiolytic-activity.

[30] M. Outirite, M. Lebrini, M. Lagrenée, F. Bentiss, New one step synthesis of 3, 5-disubstituted 1, 2, 4-oxadiazoles, J. Heterocyclic Chem. 44 (2007) 1529–1531, https://doi.org/10.1002/jhet.5570440647.

[31] N. Kaur, Microwave-assisted synthesis of five-membered O, N, N-heterocycles, Synthet. Commun. 3229–3247 (2014), https://doi.org/10.1080/00397911.2013.798666.

[32] A. Tolmachev, A.V. Bogolubsky, S.E. Pipko, A.V. Grishchenko, D.V. Ushakov, A.V. Zhemera, O.V. Iniychuk, A.I. Konovets, O.A. Zaporozhets, P.K. Mykhailiuk, Y.S. Moroz, Expanding synthesizable space of disubstituted 1, 2, 4-oxadiazoles, ACS Comb. Sci. 18 (2016) 616–624, https://doi.org/10.1021/acscombsci.6b00103.

[33] D.M. Morgan, Tetrazolium (MTT) assay for cellular viability and activity, Methods Mol. Biol. 79 (1998) 179–183 https://www.ncbi.nlm.nih.gov/pubmed/9463833.

[34] C.T. Winston, L.B. Dale, A fluorescent intercalator displacement assay for establishing DNA binding selectivity and affinity, Acc. Chem. Res. 37 (2004) 61–69, https://doi.org/10.1021/ar030113y.

[35] I. Zaki, M.K. Abdel hameid, I.M. El-Deen, A.A. Abdel Wahab, A.M. Shmawy, K.O. Mohamed, Design, synthesis and screening of 1, 2, 4-triazinone derivatives as potential antitumor agents with apoptosis inducing activity on MCF-7 breast cancer cell line, Eur. J. Med. Chem. 156 (2018) 563–579, https://doi.org/10.1016/j.ejmech.2018.07.003.